Nutrition Research 85 (2021) 99–118

Available online at www.sciencedirect.com

ScienceDirect

journal homepage: www.elsevier.com/locate/NTR

Continuous exposure to amorphous formula of curcumin from the developmental stage facilitates anti-anxiety-like behavior and fear-extinction learning in rats

Junta Nakahara[a], *Yasunori Masubuchi*[a,b], *Kazumi Takashima*[a,c], *Yasunori Takahashi*[a,c], *Ryo Ichikawa*[a], *Tomohiro Nakao*[d], *Mihoko Koyanagi*[e], *Robert R Maronpot*[f], *Toshinori Yoshida*[a,c], *Shim-mo Hayashi*[e], *Makoto Shibutani*[a,c,g,*]

[a] *Laboratory of Veterinary Pathology, Division of Animal Life Science, Institute of Agriculture, Tokyo University of Agriculture and Technology, 3-5-8 Saiwai-cho, Fuchu-shi, Tokyo 183-8509, Japan*

[b] *Pathogenetic Veterinary Science, United Graduate School of Veterinary Sciences, Gifu University, 1-1 Yanagido, Gifu-shi, Gifu 501-1193, Japan*

[c] *Cooperative Division of Veterinary Sciences, Graduate School of Agriculture, Tokyo University of Agriculture and Technology, 3-5-8 Saiwai-cho, Fuchu-shi, Tokyo 183-8509, Japan*

[d] *Emulsion Laboratory, San-Ei Gen F.F.I., Inc., 1-1-11 Sanwa-cho, Toyonaka-shi, Osaka 561-8588, Japan*

[e] *Global Scientific and Regulatory Affairs, San-Ei Gen F.F.I., Inc., 1-1-11 Sanwa-cho, Toyonaka-shi, Osaka 561-8588, Japan*

[f] *Maronpot Consulting, LLC, 1612 Medfield Road, Raleigh, NC 27607, USA*

[g] *Institute of Global Innovation Research, Tokyo University of Agriculture and Technology, 3-5-8 Saiwai-cho, Fuchu-shi, Tokyo 183-8509, Japan*

ARTICLE INFO

Article history:
Received 25 April 2020
Revised 1 October 2020
Accepted 23 October 2020

ABSTRACT

An amorphous formula of curcumin (CUR) has shown to enable an improved bioavailability after ingestion. The aim of this study was to investigate the hypothesis that exogenously administered CUR has an advantage in ameliorating post-traumatic stress disorder at low doses. To this end, Long-Evans rats were dietary exposed to CUR at 0.1% or 0.5% from gestational day 6 to postnatal day (PND) 74 or 77. Offspring exposed to 0.1% CUR revealed fa-

Abbreviations: AGIQ, α-glycosyl isoquercitrin; ARC, activity-regulated cytoskeleton-associated protein; BW, body weight; CALB2, calbindin-D-29 K; COX2, cyclooxygenase-2; C_T, threshold cycle; CUR, amorphous formula of curcumin; DAB, 3,3′-diaminobenzidine; DCX, doublecortin; EGR1, early growth response protein 1; FOS, Fos proto-oncogene, AP-1 transcription factor subunit; GABA, γ-aminobutyric acid; *Gapdh*, glyceraldehyde-3-phosphate dehydrogenase; GCL, granule cell layer; GD, gestational day; GFAP, glial fibrillary acidic protein; HPLC, high performance liquid chromatography; *Hprt1*, hypoxanthine phosphoribosyltransferase 1; IBA1, ionized calcium-binding adaptor molecule 1; IEG, immediate-early gene; IL, interleukin; LTP, long-term potentiation; mPFC, medial prefrontal cortex; NeuN, neuronal nuclei; NF-κB, nuclear factor κB; NMDA, *N*-methyl-D-aspartate; NOS, nitric oxide synthase; OFT, open field test; OLT, object location test; ORT, object recognition test; PBS, phosphate-buffered saline; PCNA, proliferating cell nuclear antigen; p-ERK1/2, phosphorylated extracellular signal-regulated kinase 1/2 (phosphorylated p44/p42 MAP kinase); PFA, paraformaldehyde; PND, postnatal day; PTSD, post-traumatic stress disorder; PVALB, parvalbumin; PVP, polyvinylpyrrolidone; ROS, reactive oxygen species; RT, reverse transcription; SGZ, subgranular zone; SOX2, SRY-box transcription factor 2; SST, somatostatin; TBR2, T-box brain protein 2; TNF-α, tumor neurosis factor alpha; TUBB3, tubulin, beta 3 class III; TUNEL, terminal deoxynucleotidyl transferase-mediated dUTP-biotin nick end-labeling.

* Corresponding author at: Laboratory of Veterinary Pathology, Division of Animal Life Science, Institute of Agriculture, Tokyo University of Agriculture and Technology, 3-5-8 Saiwai-cho, Fuchu-shi, Tokyo 183-8509, Japan, Tel./Fax: +81-42-367-5771.
E-mail address: mshibuta@cc.tuat.ac.jp (M. Shibutani).

https://doi.org/10.1016/j.nutres.2020.10.007

Keywords:
Curcumin
Amorphous formula
Anti-anxiety-like behavior
Fear extinction
Synaptic plasticity
Post-traumatic stress disorder (PTSD)

cilitation of anti-anxiety-like behavior in the open field test and fear-extinction learning tested during PND 62 to 74, increases in hippocampal granule cells expressing immediate-early gene proteins and a decrease in prelimbic cortical neurons expressing phosphorylated extracellular signal-regulated kinase 1/2 after the last trial of the fear-extinction learning test on PND 74. The constitutive gene expression levels of *Gria1*, *Gria2*, *Grin2d*, *Slc17a6*, and *Slc17a7* were altered in the hippocampal dentate gyrus and amygdala on PND 77. These results suggest alterations in synaptic plasticity to strengthen neural circuits in promoting the behavioral effects by 0.1%-CUR. In contrast, 0.5% CUR revealed a lack of any of the changes in behavioral tests that were observed at 0.1%; however, this dose upregulated oxidative stress and neuroinflammation-related genes in the hippocampal dentate gyrus, and increased neural stem cells and proliferation activity of the subgranular zone in the dentate gyrus. These results suggest a possible preventive use of CUR at low doses in mitigating some stress disorders; however, excessively absorbed doses may prevent behavioral changes by inducing neuroinflammation that affects hippocampal neurogenesis involving neural stem cells.

1. Introduction

Curcumin, a natural polyphenol contained in the rhizomes of *Curcuma longa* Linne, has pleiotropic properties such as anti-inflammatory, antioxidant, antiproliferative, and antiangiogenic activities [1]. In the brain, curcumin administration has improved hippocampal neurogenesis in chronically stressed rats [2], as well as antidepressant effects in rat depression models [3]. However, curcumin exhibits poor bioavailability because of poor absorption, rapid metabolization, and rapid systemic elimination [1]. Therefore, many methods have been proposed for improving the solubility of curcumin [4], such as amorphization, nanonization, and chemical conjugation. San-Ei Gen F.F.I., Inc. (Osaka, Japan) has recently developed an amorphous formula of curcumin (CUR) that has enabled an improved bioavailability after oral intake [5].

Classical fear conditioning is thought to contribute to anxiety disorders [6], and great efforts are being made to understand the neural circuits that underlie the acquisition, development, and disappearance of emotional memory. Three brain structures, including the medial prefrontal cortex (mPFC), hippocampus, and amygdala, form important brain circuits involved in fear conditioning and extinction [6]. The mPFC, which receives inputs from the hippocampus, projects directly onto the amygdala and midbrain, regulates the development of anxiety-like behavior and avoidance behavior against aversive stimuli [7]. There is also a prevailing notion that the prelimbic cortex, a dorsal region of the mPFC, controls the development of fear, and that the infralimbic cortex, a ventral region of the mPFC, suppresses fear [6]. The amygdala is the central brain region of fear response , and suppressive input from the mPFC is received by the basolateral amygdala and suppresses fear response by suppressing the neurons of the central nucleus of the amygdala [8].

The hippocampal dentate gyrus, known as a typical brain substructure that conducts adult neurogenesis and is responsible for memory formation and antidepressant activity, includes all processes of neuronal development of the granule cell lineage, such as self-renewal of neural stem cells, proliferation and differentiation of neural progenitor cells in the subgranular zone (SGZ), and maturation of postmitotic granule cells in the SGZ and granule cell layer (GCL) [9]. In the hilar region of the hippocampal dentate gyrus, γ-aminobutyric acid-ergic (GABAergic) interneurons connect with adult-born dentate granule cells and play a functional role in adult neurogenesis [10,11].

Synaptic plasticity is the ability of neurons to bring about changes in the connections between neuronal networks in response to use or disuse in their activity. Because memories are postulated to be represented by vastly interconnected neural circuits in the brain regions including the hippocampus [12], synaptic plasticity is an important neurochemical foundation of learning and memory [13]. Excess production of reactive oxygen species (ROS) in the hippocampus leads to detrimental effects that are involved in impairments in synaptic plasticity and memory function [14], and administration of antioxidants is effective for ameliorating cognitive deficits by protecting against oxidative damage [15].

Recently, some polyphenolic antioxidants have been shown to exert an ameliorating effect on post-traumatic stress disorder (PTSD), a trauma and stressor-related disorder, in animal models [16,17], and as a result, more attention has been given to these antioxidants. Therefore, it could be hypothesized that CUR has an advantage in ameliorating PTSD and also in strengthening other behavioral functions in normal animals at low doses. In the present study, we tested the exposure effect of CUR at lower doses than those reported with nonamorphous curcumin formula on behavioral functions of rat offspring with exposure from the gestational stage until the adult stage by setting 2 doses to observe dose responses. By means of immunohistochemistry, we evaluated the effect of CUR on synaptic plasticity changes in the GCL of the hippocampal dentate gyrus and mPFC. We also examined gene expression changes related to synaptic plasticity and chemical mediator signaling by means of real-time reverse transcription (RT)-PCR. Changes in hippocampal neurogenesis were also examined.

2. Methods and materials

2.1. Chemicals and animals

Curcumin mixed with polyvinylpyrrolidone (PVP) and sucrose fatty acid ester (amorphous formula of curcumin; curcumin content: 19.9%) and PVP and sucrose fatty acid ester (carrier solvent) were provided by San-Ei Gen F.F.I. Inc. Forty-one mated female Iar: Long-Evans rats were purchased from Japan SLC, Inc. (Hamamatsu, Japan) at gestational day (GD) 3, where GD 0 is the day the appearance of vaginal plug. Rats were individually housed with their offspring in polycarbonate cages with paper bedding until postnatal day (PND) 21, where PND 0 was defined as the day of delivery. Animals were kept in an air-conditioned animal room (temperature: 23 ± 2 °C, relative humidity: 55 ± 15%) with a 12-h light/dark cycle. Mated female rats were provided ad libitum a commercial rodent powder diet (CRF-1; Oriental Yeast Co., Ltd., Tokyo, Japan) until exposure to CUR began on GD 6 and tap water during the experiment.

While the detailed ingredient composition of the CRF-1 is not available (commercial formulation), this diet was mainly formulated from corn, wheat (bran), defatted soybeans, defatted rice bran, alfalfa, fish flour, skim milk powder, soybean oil, and brewer's yeast. The macronutrient composition of the CRF-1 is 8.2% moisture, 21.9% crude protein, 5.4% crude fat, 6.3% crude ash, 2.9% crude fiber, 55.3% nitrogen-free extract, and total energy of 3570 kcal/kg. Vitamin content/kg was as follows: vitamin A, 32,450 IU; vitamin D3, 6430 IU; vitamin E, 203 mg; vitamin K3, 1.6 mg; vitamin B1, 47.4 mg; vitamin B2, 33.1 mg; vitamin C, 120 mg; vitamin B6, 12.7 mg; vitamin B12, 172 μg; inositol, 4530 mg; biotin, 271 μg; pantothenic acid, 50.7 mg; niacin, 156.2 mg; choline, 2.6 g; folic acid, 2.7 mg. Mineral content/kg is as follows: calcium, 12.2 g; phosphorus, 8.1 g; magnesium, 2.3 g; sodium, 2.6 g; potassium, 8.6 g; iron, 138 mg; aluminum, 21 mg; cupper, 9.5 mg; zinc, 61.5 mg; cobalt, 3.3 mg; manganese, 72.7 mg. Amino acid content/kg is as follows: isoleucine, 8.2 g; leucine, 16.1 g; lysine, 11.2 g; methionine, 4.4 g; cysteine, 3.4 g; phenylalanine, 9.6 g; tyrosine, 6.4 g; threonine, 8.3 g; tryptophan, 2.7 g; valine, 10.2 g; arginine, 13.0 g; histidine, 5.6 g; alanine, 11.3 g; aspartic acid, 19.2 g; glutamic acid, 37.5 g; glycine, 11.0 g; proline, 12.6 g; serine, 10.3 g.

From PND 21 onward, offspring were reared and provided the CRF-1 diet with or without CUR and tap water ad libitum throughout the experimental period. Dietary concentration of curcumin was measured using the diets kept for 17 days after preparation of 0.1% and 0.5% in diet by high performance liquid chromatography (HPLC; analyzed by San-Ei Gen F.F.I., Inc.), and the same concentration of curcumin was confirmed in diet after the preservation.

2.2. Experimental design

Mated female rats were randomly divided into three groups of vehicle controls (14 animals), 0.1% CUR (13 animals) and 0.5% CUR (14 animals) (Fig. 1). These animals were treated from GD 6 to day 21 post-delivery with PVP and sucrose fatty acid ester at 1.95 w/w% (vehicle controls), curcumin at 0.1 w/w% with 0.39 w/w% vehicle (0.1% CUR), or curcumin at 0.5 w/w% with 1.95 w/w% vehicle (0.5% CUR) in the basal diet (Table 1). Considering 5.7-fold higher absorption rate than nonamorphous fine-particulate formula of curcumin calculated by $AUC_{0\ to\ 24\ hours}$ after single oral administration of 100 mg/kg body weight (BW) [18], the doses of CUR were determined based on the study results of nonamorphous formula of curcumin with the dietary dose at 1.5% that impaired fear memory consolidation and reconsolidation by treatment for 5 days in a PTSD-induction model using rats [19]. In the present study, the rationale for setting the dose levels of CUR was to examine continuous exposure effect of CUR from fetal stages with the doses lower than nonamorphous curcumin formula, and therefore, we set 2 doses, 1 lower than and the other higher than the absorbed value of 1.5% dietary dose of aforementioned nonamorphous formula of curcumin. Concentrations of curcumin in plasma removed from male offspring cardiac blood on PND 21 ($N = 8$ each from the vehicle controls and 0.5% CUR) and in milk from female offspring stomach on PND 14 ($N = 8$ each from the vehicle controls and 0.5% CUR) were measured using HPLC by Japan Food Research Laboratories (Tokyo, Japan). For measuring curcumin concentrations in milk, one dam each from the vehicle controls and 0.5% CUR was used.

Table 1 – Composition of the experimental diets fed to rats

	g/kg		
	Ctrl	0.1% CUR [a]	0.5% CUR
Basal diet	980.5	995.0	974.8
Curcumin powder	0	1.1	5.7
Polyvinylpyrrolidone	13.2	2.6	13.2
Sucrose fatty acid ester	6.3	1.3	6.3

Abbreviations: Ctrl, vehicle controls; CUR, amorphous formula of curcumin.

[a] Curcumin-containing diets were prepared by adding the amorphous formula of curcumin, a mixture of curcumin powder with polyvinylpyrrolidone and sucrose fatty acid ester as a carrier solvent (curcumin content: 19.9%), to the basal diet. Basal diet was mixed with vehicle at 1.95 w/w% for vehicle controls, curcumin at 0.1 w/w% with 0.39 w/w% vehicle for 0.1% CUR, or curcumin at 0.5 w/w% with at 1.95 w/w% vehicle for 0.5% CUR.

Dams were subjected to measurement of BW and food and water consumption twice a week from GD 6 to day 21 post-delivery. On PND 4, litters were randomly culled to preserve 7 or 8 male and 0 or 1 female pups per dam. If dams had fewer than 7 male pups, more female pups were included to maintain a total of 8 pups per litter. The offspring were weighed twice a week until PND 21. Dams were euthanized by exsanguination from the abdominal aorta under CO_2/O_2 anesthesia on day 21 post-delivery. In this study, male offspring were selected for behavioral tests and immunohistochemical and gene expression analyses because animal behaviors and hippocampal neurogenesis are influenced by circulating levels of steroid hormones during the estrous cycle [20,21].

On PND 21, 28 to 35 male offspring (1-2 pups per dam) and all female offspring of all groups were euthanized by exsanguination from the abdominal aorta under CO_2/O_2-induced anesthesia and subjected to necropsy for brain tissue sampling for other purposes of analysis. The remaining male

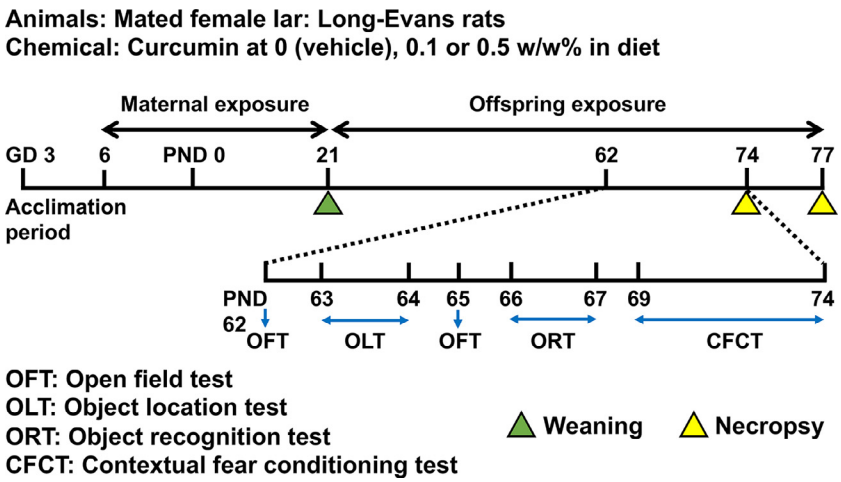

Fig. 1 – Experimental design of continuous exposure to amorphous formula of curcumin from developmental stage in rats.

offspring were fed a diet containing CUR or vehicle at the same concentration to dams until PND 77 (4 or 5 animals/cage during PND 21-PND 40; 2 or 3 animals/cage from PND 41 onwards); BW and food and water consumption were measured once weekly. Behavioral tests were performed using 10 to 26 male offspring per group (1-2 pups per dam) during the period from PND 62 to PND 74.

On PND 74, animals that were subjected to behavioral tests were euthanized for brain sampling. Ten male offspring per group (1 pup per dam) were subjected to perfusion fixation for brain immunohistochemistry through the left cardiac ventricle with ice-cold 4% (w/v) paraformaldehyde (PFA) in 0.1 M phosphate buffer (pH 7.4) at a flow rate of 35 mL/min under CO_2/O_2-induced anesthesia. For transcript-level expression analysis, brain samples from 6 male offspring per group (1 male offspring per dam) were prepared. Animals were sacrificed at 90 min after the 3rd trial of fear-extinction learning.

On PND 77, animals that were not subjected to behavioral tests were euthanized for brain sampling. Ten male offspring per group (1 male offspring per dam) were subjected to perfusion fixation for brain immunohistochemistry in the same way with PND 74 samples. For transcript-level expression analysis of constitutive expression changes, brain samples from 6 male offspring per group (1 male offspring per dam) were prepared.

All dams and offspring were checked each day to assess their general appearance (abnormal gait and behaviors). All procedures in this study were conducted in accordance with the National Institutes of Health guide for the care and use of laboratory animals (NIH Publications No. 8023, revised 1978) and according to the protocol approved by the Animal Care and Use Committee of The Tokyo University of Agriculture and Technology (Approved No.: 30–63). All efforts were made to minimize animal suffering.

2.3. *Behavioral tests*

In each behavioral test, male animals were transported from the animal room to the behavioral test room 1 hour to 2 hours before starting the tests. After the end of each behavioral test, animals were promptly returned to the home cage and transferred to the animal room. Apparatuses were cleaned with 70% ethanol solution before and after each test. All experiments were conducted during the period from 8:00 am to 7:00 p.m., and the order of animal selection for tests among groups was counter-balanced across test time to avoid any bias in the trial times of each group.

2.3.1. *Open field test (OFT)*

The OFT was performed on PND 62 and PND 65 to assess locomotor activity and anxiety-like behaviors and to habituate the animals to the arena as an acclimation phase in the object location test (OLT) and object recognition test (ORT) on the following days. Two pups from one dam were assigned to OFT. The arena comprised a square stainless-steel tray with a matte black polyvinyl plastic surface and stainless-steel walls with matte black polyvinyl plastic surface surrounding the tray (900 mm width × 900 mm depth × 500 mm height; O'Hara & Co., Ltd., Tokyo, Japan). The illumination was set at 20 Lux at the middle of the arena. Each animal was placed at the corner of the arena with the head facing the wall and allowed to explore the arena freely for 10 min. Time spent in the central region (540 mm × 540 mm) or wall side and the total distance moved were recorded by a CCD camera (WAT-902B; Watec Co., Ltd., Tsuruoka, Japan) mounted above the arena and evaluated by an automatic video-tracking system (TimeOFCR1 software; O'Hara & Co. Ltd.).

2.3.2. *Object location test and object recognition test*

The OLT was performed on PND 63 and PND 64 to assess spatial object memory, and the ORT was performed on PND 66 and PND 67 to assess nonspatial object memory. All experiments in both tests were conducted in the same arena that was used in the OFT. One different pup from one dam was assigned to each of OLT and ORT. Both of the OLT and ORT comprised three steps: acclimation, sample phase, and test phase. As aforementioned, OFT was conducted as acclimation of animals in both of the OLT and ORT. After 24 hours, each animal was placed in the middle of the wall along the inside of the field with the head facing the wall and allowed to explore for 5

min with 2 identical sample objects (sample phase in the OLT and ORT). Objects were placed equidistant to this location to the right and left sides behind the animal in the arena. Test phase of the OLT and ORT was conducted 24 hours after the sample phase, and the animals were placed in the same position as the sample phase. In the OLT, each animal was allowed to explore for 3 min with one object on the same location and the other object moved to the opposite side of the arena. In this experiment, objects were identical to the sample phase, and the position of one of the two objects was displaced 35 cm away from the original position. In the ORT, each animal was allowed to explore for 3 min with one sample object and one novel object on the same location as sample phase. The illumination was set at 20 Lux on the middle of the arena. The sample object was a gray cone of polyvinyl plastic with a rough surface and a stainless-steel tip. The novel object was a sphere with a patchy pattern of black and white consisting of smooth polyvinyl plastic. These objects were heavy enough that could not to be moved by the animals. In both of the sample and test phases, the total distance traveled and exploration time toward each object were recorded by a CCD camera (WAT-902B; Watec Co., Ltd.) mounted above the arena and evaluated by automatic video-tracking system (TimeSSI software; O'Hara & Co., Ltd.). When a rat's nose approached to within 3 cm of an object, the video-tracking system automatically counted it as "exploration" and the cumulative exploration time was recorded.

A discrimination index for the OLT or ORT was determined using the following formula: discrimination index = exploration time with displaced object or novel object/(exploration time with familiar object + exploration time with displaced object or novel object).

2.3.3. *Contextual fear conditioning test*

The contextual fear conditioning test was performed during PND 69 and PND 74 using all the animals subjected to OFT, OLT, and ORT. Conditioning and testing took place in a rodent observation cage (370 mm width × 300 mm depth, 250 mm height; CL-3001, O'Hara & Co., Ltd.) that was placed in a sound-attenuating chamber (CL-4211; O'Hara & Co., Ltd.). The sidewalls and door of the observation cage were constructed of Plexiglas. The floor comprised 21 steel rods through which a scrambled footshock from a shock generator (SGA-2020; O'Hara & Co., Ltd.) could be delivered. During experiments, the chamber was ventilated, kept at a background white noise level of 50 dB, and illuminated at 200 Lux by white light emitting diode bulbs. This test comprised four steps: habituation, contextual fear conditioning, fear acquisition, and fear extinction.

Habituation (Day 1): To familiarize with test surroundings, animals were placed into the observation cage for 5 min without footshock.

Contextual fear conditioning (Day 2): Twenty-four hours after the habituation, each animal was moved to the observation cage, and after 88, 148, and 238 sec, they received 2 sec footshocks (0.3 mA intensity, a total of 3 footshocks). Animals were removed from the observation cage 60 sec after the final footshock and returned to the home cage. Thus, it took 5 min for a test.

Fear acquisition (Day 3): Twenty-four hours after the conditioning, each animal was placed back into the same context as the conditioning context for 5 min without footshock.

Fear extinction (Day 4, 5, 6): After 2, 3, and 4 days of the conditioning, each animal was placed back into the same context as the conditioning context for 5 min without footshock.

The animals' behavior was video recorded by the CCD camera (WAT-902B; Watec Co., Ltd.) mounted above the observation cage and analyzed using an automatic video-tracking system (TimeFZ2 software; O'Hara & Co., Ltd.). Body freezing time was automatically measured, and the freezing time was defined as the percent of time the rat spent in freezing behavior for ≥ 5 sec during each of the experiment time of 5 min.

2.4. *Immunohistochemistry and apoptotic cell detection*

For immunohistochemistry analysis, perfusion-fixed brains of male offspring were additionally fixed with the same PFA buffer solution overnight. Coronal cerebral slices were prepared at +3.0 mm and –3.5 mm from the bregma of the brains at PND 74 and PND 77 (N = 9-10/group) using a brain-matrix cast (Muromachi Kikai Co., Ltd., Tokyo, Japan). Due to a mistake in slicing at +3.0 mm, one sample each of the vehicle controls and 0.1% CUR was excluded from counting of immunoreactive cells. Brain slices were further immersion-fixed with the same PFA buffer solution overnight at 4°C and were routinely processed for paraffin embedding and sliced into 3-μm-thick sections.

Brain sections were subjected to immunohistochemical analysis using primary antibodies against the following (Table 2): Glial fibrillary acidic protein (GFAP), which is expressed in type-1 neural stem cells (radial glial cells) in the SGZ and astrocytes [9]; SRY-box transcription factor 2 (SOX2), which is expressed in type-1 neural stem cells and type-2a progenitor cells in the SGZ [9]; T-box brain protein 2 (TBR2), expressed in type-2b progenitor cells in the SGZ [9]; doublecortin (DCX), which is expressed in type-2b and type-3 progenitor cells and immature granule cells in the SGZ and GCL [9]; tubulin, beta 3 class III (TUBB3, also known as Tuj-1), which is expressed mainly in postmitotic immature granule cells in the SGZ and GCL [22]; neuronal nuclei (NeuN), which is expressed in postmitotic neurons of both immature and mature granule cells in the SGZ and GCL [9]; and parvalbumin (PVALB), calbindin-D-29 K (CALB2), and somatostatin (SST), which are expressed in GABAergic interneurons [10]; Ionized calcium-binding adaptor molecule 1 (IBA1), a microglia-specific molecule in the brain [23]; proliferating cell nuclear antigen (PCNA), a cell proliferation marker; Fos proto-oncogene, AP-1 transcription factor subunit (FOS), activity-regulated cytoskeleton-associated protein (ARC), cyclooxygenase-2 (COX2), early growth response protein 1 (EGR1, also known as Zif268), which are members of the immediate-early gene (IEG) proteins involved in synaptic plasticity [13]; phosphorylated extracellular signal-regulated kinase 1/2 (p-ERK1/2; phosphorylated p44/p42 MAP kinase), a member of the mitogen activated protein kinase family that is activated by phosphorylation to promote transcriptional programs leading to the induction of *Arc, Fos,* and *Egr1* [24,25].

Table 2 – Antibodies used in this study

Antigen	Abbreviated name	Host species	Clonality	Clone name	Dilution	Antigen retrieval	Manufacturer (city, state, country)
Activity-regulated cytoskeleton-associated protein	ARC	Rabbit	Polyclonal IgG	n.a.	1:2000	Microwaving[a]	Synaptic Systems GmbH (Goettingen, Germany)
Calbindin-D-29K	CALB2	Rabbit	Monoclonal IgG	EP1798	1:600	Microwaving[a]	Abcam plc (Cambridge, UK)
Cyclooxygenase-2	COX2	Mouse	Monoclonal IgG_1	33/Cox-2	1:200	Microwaving[a]	BD Biosciences, Inc. (San Jose, CA, USA)
Doublecortin	DCX	Rabbit	Polyclonal IgG	n.a.	1:1000	None	Abcam plc
Early growth response protein 1	EGR1	Rabbit	Monoclonal IgG	15F7	1:200	Microwaving[a]	Cell Signaling Technology, Inc. (Danvers, MA, USA)
Fos proto-oncogene, AP-1 transcription factor subunit	FOS	Rabbit	Polyclonal IgG	n.a.	1:500	None	Santa Cruz Biotechnology, Inc. (Dallas, TX, USA)
Glial fibrillary acidic protein	GFAP	Mouse	Monoclonal IgG_1	GA5	1:200	None	Merck Millipore (Burlington, MA, USA)
Ionized calcium-binding adaptor molecule 1	IBA1	Rabbit	Polyclonal IgG	n.a.	1:300	None	Fujifilm Wako Pure Chemical Corporation (Osaka, Japan)
Neuronal nuclei	NeuN	Mouse	Monoclonal IgG_1	A60	1:100	None	Merck Millipore
Parvalbumin	PVALB	Mouse	Monoclonal IgG_1	PARV-19	1:1000	Microwaving[a]	Merck Millipore
phosphorylated extracellular signal-regulated kinase 1/2 (phosphorylated p44/p42 MAP kinase)	p-ERK1/2	Rabbit	Monoclonal IgG	137F5	1:100	Microwaving[a]	Cell Signaling Technology, Inc.
Proliferating cell nuclear antigen	PCNA	Mouse	Monoclonal IgG_{2a}	PC10	1:200	None	Agilent Technologies (Santa Clara, CA, USA)
SRY-box transcription factor 2	SOX2	Mouse	Monoclonal IgG_1	9–9–3	1:4000	None	Abcam plc
Somatostatin	SST	Rabbit	Polyclonal IgG	n.a.	1:400	Microwaving[a]	Abcam plc
T box brain 2	TBR2	Rabbit	Polyclonal IgG	n.a.	1:500	Autoclaving[b]	Abcam plc
Tubulin, beta 3 class III	TUBB3	Mouse	Monoclonal IgG_1	TU-20	1:500	Microwaving[a]	Abcam plc

Abbreviation: n.a, not applicable.
[a] 90°C for 10 min in 10 mM citrate buffer (pH 6.0).
[b] 121°C for 10 min in 10 mM citrate buffer (pH 6.0).

Immunodetection was conducted using a Vectastain *Elite* ABC kit (Vector Laboratories Inc., Burlingame, CA, USA). In detail, paraffin-embedded brain sections were deparaffinized in xylene, rehydrated in a graded ethanol series and immersed in a tap water. The antigen retrieval was applied for some antibodies and the retrieval conditions are listed in Table 2. Endogenous peroxidase was blocked by exposure to 0.3% (v/v) H_2O_2 solution in absolute methanol for 30 min and sections were rinsed in phosphate-buffered saline (PBS; pH 7.4). Blocking was conducted with 1.5% normal serum in PBS for 30 min. Horse serum was used in case of mouse monoclonal primary antibodies and goat serum was used for rabbit monoclonal and polyclonal primary antibodies. Incubation with respective primary antibodies was performed at 4 °C overnight. All antibodies were diluted with PBS containing 0.5% casein. This step was followed by incubation with: (a) Biotinylated horse antimouse secondary antibody or biotinylated goat antirabbit secondary antibody in PBS containing 1.5% normal serum for

30 min; (b) peroxidase-conjugated avidin in PBS for 30 min. After each step, the sections were rinsed in PBS and all steps except for incubation with primary antibody were performed at room temperature. All incubations were performed in a humidity chamber. Peroxidase activity was visualized by reaction with freshly prepared 0.03% 3,3′-diaminobenzidine (DAB) plus 0.01% hydrogen peroxide in Tris-buffered saline (pH 7.6). Hematoxylin counterstaining was then performed, and coverslips were mounted on immunostained sections for microscopic examination. One section per animal was subjected to immunohistochemistry of each molecule.

To evaluate apoptosis in the SGZ of the dentate gyrus in the offspring, terminal deoxynucleotidyl transferase-mediated dUTP-biotin nick end-labeling (TUNEL) assay was performed using the ApopTag Peroxidase *In Situ* Apoptosis Detection Kit (Merck Millipore, Burlington, MA, USA) according to the manufacturer's instructions, with DAB/H_2O_2 as the chromogen. One section per animal was subjected to TUNEL assay.

2.5. *Evaluation of immunoreactive cells and apoptotic cells*

Immunoreactive cells (GFAP$^+$, SOX2$^+$, TBR2$^+$, DCX$^+$, TUBB3$^+$, NeuN$^+$, FOS$^+$, ARC$^+$, COX2$^+$, EGR1$^+$, p-ERK1/2$^+$, and PCNA$^+$ cells) or TUNEL$^+$ apoptotic cells in the SGZ and/or GCL were bilaterally counted and normalized for the length of the SGZ (Fig. 2). Immunoreactive cells (PVALB$^+$, CALB2$^+$, SST$^+$, GFAP$^+$ and IBA1$^+$ cells) distributed within the hilus of the hippocampal dentate gyrus were bilaterally counted and normalized per area unit of the hilus area (Fig. 2). Immunoreactive neurons located inside of the Cornu Ammonis region 3, consisting of large pyramidal neurons that can be morphologically distinguished from relatively small interneurons, were excluded from counting immunoreactive cells in the hilus of the dentate gyrus. Immunoreactive cells (FOS$^+$, ARC$^+$, COX2$^+$, and p-ERK1/2$^+$ cells) in the infralimbic cortex and prelimbic cortex of the mPFC were bilaterally counted and normalized per area unit of each cortical area (Fig. 3). The position and shape of each area were determined with reference to a cresyl violet staining image adjacent to the immunostained sections and the atlas of the rat brain [26].

Brain samples of animals that were subjected to behavioral analysis and euthanized on PND 74 were examined for immunohistochemistry of FOS, ARC, COX2, EGR1, and p-ERK1/2. Because expression peak of IEG proteins in response to acute stimuli occurs within approximately 90 to 120 min [27], animals were euthanized for perfusion fixation 90 min after the last trial of the contextual fear conditioning test. Brain samples of animals that were not subjected to behavioral analysis and euthanized on PND 77 were examined for immunohistochemistry of GFAP, SOX2, TBR2, DCX, TUBB3, NeuN, PCNA, PVALB, CALB2, SST and IBA1, as well as FOS and ARC, and for TUNEL assay.

The number of each immunoreactive cellular population (except for NeuN$^+$ cells in the GCL) or TUNEL$^+$ apoptotic cells was manually counted while blinded to the treatment conditions under microscopic observation using a BX53 microscope (Olympus Corporation, Tokyo, Japan). In case of GFAP$^+$ cells in the SGZ, only those having apparent vertically extending radial processes were counted as type-1 neural stem cells. In case of NeuN$^+$ cells in the GCL, the number of immunoreactive cells for counting was high, and therefore, an image analysis-assisted automatic cell counting method was applied. More specifically, digital photomicrographs at × 200-fold magnification were taken using a DP72 Digital Camera System (Olympus Corporation), attached to a BX53 microscope, and positive cell counting was performed applying the WinROOF image analysis software package (version 5.7; Mitani Corporation, Fukui, Japan). The length of the SGZ and the hilar area were measured in microscopic images at × 40-fold magnification by applying the cellSens Standard (version 1.9; Olympus Corporation).

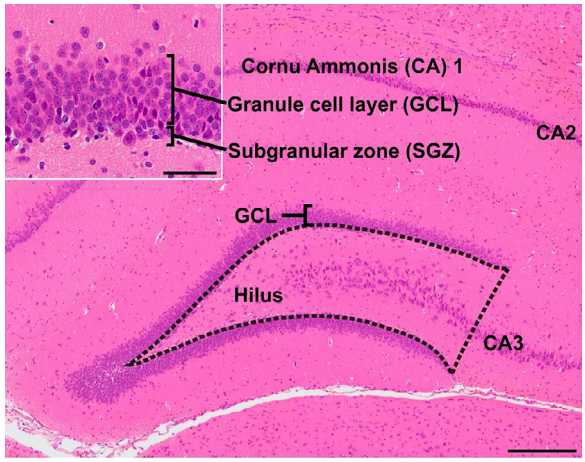

Fig. 2 – Overview of the hippocampal formation of a male rat stained with hematoxylin and eosin. (Inset) Higher magnification of the granule cell layer (GCL) and subgranular zone (SGZ). The distribution of immunoreactive cells for GFAP, SOX2, TBR2, DCX, TUBB3, NeuN, ARC, FOS, COX2, EGR1, p-ERK1/2, and proliferating cells or apoptotic cells were measured in the SGZ and/or GCL. The number of cells in the hilus of the dentate gyrus (as enclosed by the dotted line) displaying immunoreactivity for PVALB, SST, CALB2, GFAP or IBA1 was counted and normalized for the unit area. Only small-sized cells with positive immunoreactivity for these antigens were counted, and larger Cornu Ammonis (CA) 3 neurons were excluded from counting. Magnification × 40; bar 250 μm. (Inset) Higher magnification of the GCL. Magnification × 400; bar 50 μm.

2.6. *Transcript-level expression analysis*

Transcript levels in the hippocampal dentate gyrus, amygdala, infralimbic cortex and prelimbic cortex were examined using real-time RT-PCR in male offspring. Brain tissues were dissected according to the whole-brain fixation method using methacarn solution as previously reported [28]. In brief, 2-mm coronal cerebral slices were prepared at −3.0 mm from the bregma using a brain-matrix cast to collect tissue samples from the hippocampal dentate gyrus and amygdala using a punch-biopsy device with a pore-size diameter of 1 mm in diameter (BP-10F; Kai Industries Co., Ltd., Gifu, Japan) (Fig. 4). For sampling the infralimbic cortex and prelimbic cortex tissues, 2-mm-thick coronal cerebral slices were prepared

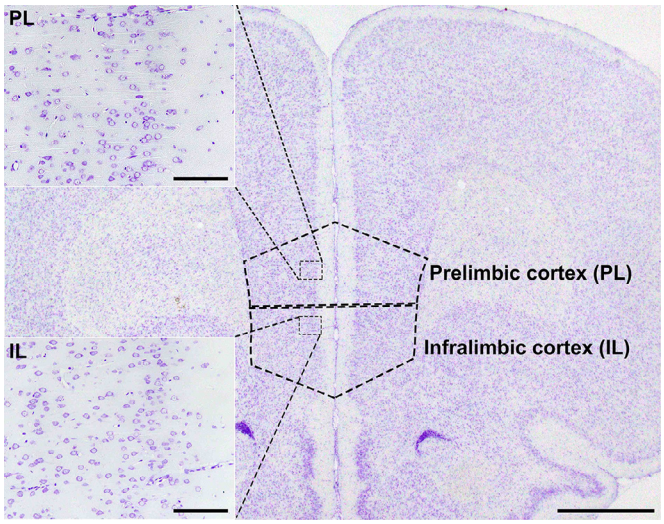

Fig. 3 – Overview of the medial prefrontal cortex formation of a male rat stained with cresyl violet. (Inset) Higher magnification of the prelimbic cortex (PL) and infralimbic cortex (IL). The distribution of immunoreactive cells for ARC, FOS, COX2, and p-ERK1/2 were measured in the PL and IL. Magnification × 12.5; bar 1 mm. (Inset) Higher magnification of the PL or IL. Magnification × 200; bar 100 μm.

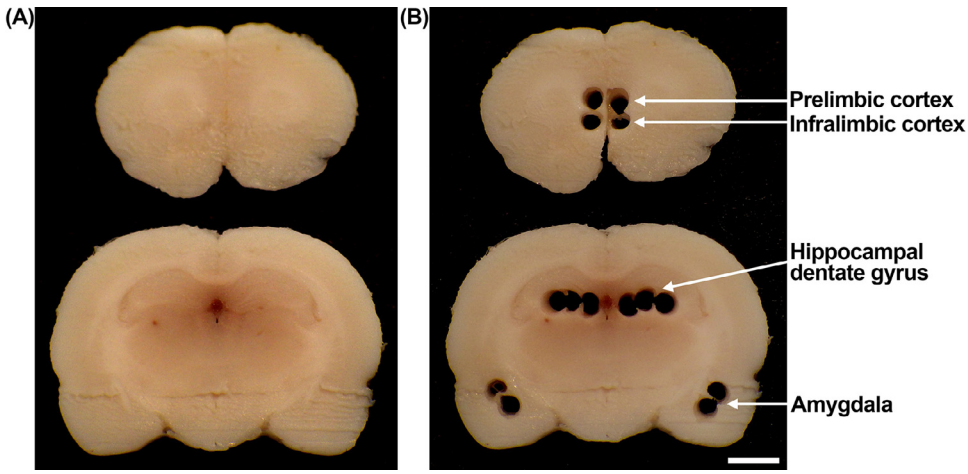

Fig. 4 – Overview of the dissected brain regions for transcript-level expression analysis of rat offspring. Sampling was made from methacarn-fixed brain tissue slices using punch-biopsy devices bilaterally. For sampling of the tissues of the infralimbic cortex and prelimbic cortex, a 2 mm-thick slice anterior to the coronal cerebral plane at +2.0 mm from the bregma was prepared. For sampling of the tissues of the hippocampal dentate gyrus and amygdala, a 2 mm-thick slice posterior to the −2.0 mm coronal plane from the bregma was prepared. (A) The coronal cut surface views at +3.0 mm and −3.0 mm from the bregma before dissection. (B) The identical surface view to the panel (A) after dissection of the prelimbic cortex, infralimbic cortex, hippocampal dentate gyrus and amygdala. Bar 2 mm.

at +2.0 mm from the bregma. Total RNA was extracted from brain tissue samples from all groups ($n = 6$ per group) using RNeasy Mini kit (Qiagen, Hilden, Germany). First-strand cDNA was synthesized using SuperScript III Reverse Transcriptase (Thermo Fisher Scientific, Waltham, MA, USA) in a 20-μL total reaction mixture with 1 μg of total RNA. Analysis of the transcript levels for the gene targets shown in Table 3 was performed using PCR primers designed with Primer Express software (Version 3.0; Thermo Fisher Scientific). Real-time PCR with Power SYBR Green PCR Master Mix (Thermo Fisher Scientific) was conducted using a StepOnePlus Real-time PCR System (Thermo Fisher Scientific). The relative differences in gene expression between the vehicle controls and each exposure group were calculated using threshold cycle (C_T) values that were first normalized to that of glyceraldehyde-3-phosphate dehydrogenase (*Gapdh*) or hypoxanthine phosphoribosyltransferase 1 (*Hprt1*), which served as endogenous controls in the same sample, and then relative to a control C_T value using the $2^{-\Delta\Delta C_T}$ method [29].

Transcript levels of all genes were measured in the hippocampal dentate gyrus using samples of PND 77 animals that were not subjected to behavioral tests, except for *Il1a*, *Il1b*, *Il4*,

Table 3 – Sequence of primers used for real-time RT-PCR

Gene	Accession no.	Forward primer (5′ → 3′)	Reverse primer (5′ → 3′)
Glutamate receptors			
Gria1	NM_031608	GTGAGCGTCG TCCTCTTCCT	TCTTCGCTGT GCCATTCGTA
Gria2	NM_001083811.1	CATCACACCT AGCTTCCCAA CA	CTTTGAGGTC AGGTCGCATC T
Gria3	NM_032990	GAAACATAAA GGACGTCCAG GAA	TTCCTGCCTT CTGTCCATTT CT
Grin2a	NM_012573	GGCTGTCAGC ACTGAATCCA	GGTTTAGAGA ATCCTGGCGT AGAG
Grin2b	NM_012574	TCGTCAAGAC ACAAGATTA AAACCA	GGAGGATAAA GGAACGGAAG AAA
Grin2c	NM_012575.3	TGGGTGATGA TGTTCGTGAT G	GTGAGGTTCT GGTTGTAGCT GACA
Grin2d	NM_022797	TCGTGCTCAC ACCCAAGGA	GGTCACTGCC ACAAAGGATG T
Glutamate transporters			
Slc17a6	NM_053427.1	GGCAGACCCT GAGGAAACAA	TCCCCCGTTT CTTCATCCA
Slc17a7	NM_053859.2	TTGTGGCTAC CTCCACCCTA A	CGAAGATGAC ACAGCCATAG TGA
Synaptic plasticity-related genes			
Fos	NM_022197	CAACGAGCCC TCCTCTGACT	TGCCTTCTCT GACTGCTCAC A
Jun	NM_021835	CTAACCCCGC GTGAAGTGA	GCATCGTCGT AGAAGGTCGT TT
Arc	NM_019361.1	AGTGTCTGAA AGGCAATGAA AAGTAG	CCTTCGGCCA TCTCTGATTC
Ptgs2	NM_017232.3	GCTTTCTCCA ACCTCTCCTA CTACA	GGGAGTTGGG CAGTCATCAG
Egr1	NM_012551.2	CGAGCGAACA ACCCTACGA	CGTTATTCAG AGCGATGTCA GAA
Oxidative stress-related genes			
Nfe2l2	NM_031789	TGCCCCTGGA AGTGTCAAA	GGCTGTACTG TATCCCCAGA AGA
Keap1	NM_057152	CAGAACAAGC CATGCCTTCT T	TCTGGTCTTC CACAAGGTCC TT
Nos1	NM_052799.1	TCCAATGTTC ACAAAAAACG AGTCT	TCGGCTGGAC TTAGGGCTTT
Nos2	NM_012611.3	GGATTTTCCC AGGCAACCA	ACAATCCACA ACTCGCTCCA A
Nos3	NM_021838.2	CACCAGGAAG AAGACTTTTA AGGAA	CACACGCTTC GCCATCAC
Chemical mediators and related molecules			
Nfkb1	NM_001276711.1	CACTAAATCC AACACAGGCA TCAC	GGCACAATCT CTAGGCTCGT TT
Il1a	NM_017019.1	GAGGCCATAG CCCATGATTT AG	TGGAAGCTGT GAGGTGCTGA T
Il1b	NM_031512	TGACAGACCC CAAAAGATTA AGG	CTCATCTGGA CAGCCCAAGT C
Il4	NM_201270	CAAATTTTAC TTCCCACGTG ATGT	CACCGAGAAC CCCAGACTTG
Il6	NM_012589	GAGGATACCA CTCCCAACAG ACC	AAGTGCATCA TCGTTGTTCA TA
Tnf	NM_012675.3	GCCCGAGGCA ACACATCT	CCAGTTCCAC ATCTCGGATC A
Interneuron marker genes			
Pvalb	NM_022499	TCGCCACAAA AAGTTCTTCC A	TCTTCACATC ATCCGCACTC TT
Calb2	NM_053988	AGCTCCAGGA GTACACCCAA AC	CCCAATTTGC CGTCTCCAT
Sst	NM_012659.1	ACCCCGGGAA CGCAAA	CAGGATGTGA ATGTCTTCCA GAAG
Reln	NM_080394	GCCAGCTTTC GACTACCCTA TTAAC	CGTAGTGGCA CAGAAGCTAT CG
Normalization control genes			
Gapdh	NM_017008	GGCCGAGGGC CCACTA	TGTTGAAGTC ACAGGAGACA ACCT
Hprt1	NM_012583	GCCGACCGGT TCTGTCAT	TCATAACCTG GTTCATCATC ACTAATC

Abbreviations: *Arc*, activity-regulated cytoskeleton-associated protein; *Calb2*, calbindin 2 (also known as calbindin-D-29K); *Egr1*, early growth response protein 1; *Fos*, Fos proto-oncogene, AP-1 transcription factor subunit; *Gapdh*, glyceraldehyde-3-phosphate dehydrogenase; *Gria1*, glutamate ionotropic receptor AMPA type subunit 1; *Gria2*, glutamate ionotropic receptor AMPA type subunit 2; *Gria3*, glutamate ionotropic receptor AMPA type subunit 3; *Grin2a*, glutamate ionotropic receptor NMDA type subunit 2A; *Grin2b*, glutamate ionotropic receptor NMDA type subunit 2B; *Grin2c*, glutamate ionotropic receptor NMDA type subunit 2C; *Grin2d*, glutamate ionotropic receptor NMDA type subunit 2D; *Hprt1*, hypoxanthine phosphoribosyltransferase 1; *Il1a*, interleukin 1 alpha; *Il1b*, interleukin 1 beta; *Il4*, interleukin 4; *Il6*, interleukin 6; *Jun*, Jun proto-oncogene, AP-1 transcription factor subunit; *Keap1*, Kelch-like ECH-associated protein 1; *Nfe2l2*, nuclear factor, erythroid 2-like 2; *Nfkb1*, nuclear factor kappa B subunit 1; *Nos1*, nitric oxide synthase 1; *Nos2*, nitric oxide synthase 2; *Nos3*, nitric oxide synthase 3; *Ptgs2*, prostaglandin-endoperoxide synthase 2; *Pvalb*, parvalbumin; *Reln*, reelin; RT-PCR, reverse transcription-polymerase chain reaction; *Slc17a6*, solute carrier family 17 member 6; *Slc17a7*, solute carrier family 17 member 7; *Sst*, somatostatin; *Tnf*, tumor necrosis factor.

and *Il6* examined using samples of PND 74 animals that were subjected to behavioral tests. In the amygdala, prelimbic cortex and infralimbic cortex, transcript levels of genes encoding glutamate receptors and transporters were measured using samples of PND 77 animals.

2.7. *Statistical analyses*

Maternal data, such as BWs, food and water consumption were analyzed using the individual animal as the experimental unit. Offspring data, such as body and brain weights at necropsy, the number of immunoreactive cells for each antigen, number of apoptotic cells, and the transcript-level expression data, were analyzed using the litter as the experimental unit.

Because some animals were resistant to fear-extinction learning, the Smirnov-Grubbs test was performed to detect the outliers in each group. Identified outliers were excluded as abnormal animals from the fear-extinction test analysis. The Smirnov-Grubbs test was performed using Excel Statistics 2013 software package version 2.02 (Social Survey Research Information Co. Ltd., Tokyo, Japan).

Data were analyzed using Levene's test for homogeneity of variance. If the variance was homogenous, numerical data were evaluated using Dunnett's test for comparisons between the vehicle controls and 0.1% CUR or 0.5% CUR. For heteroge-

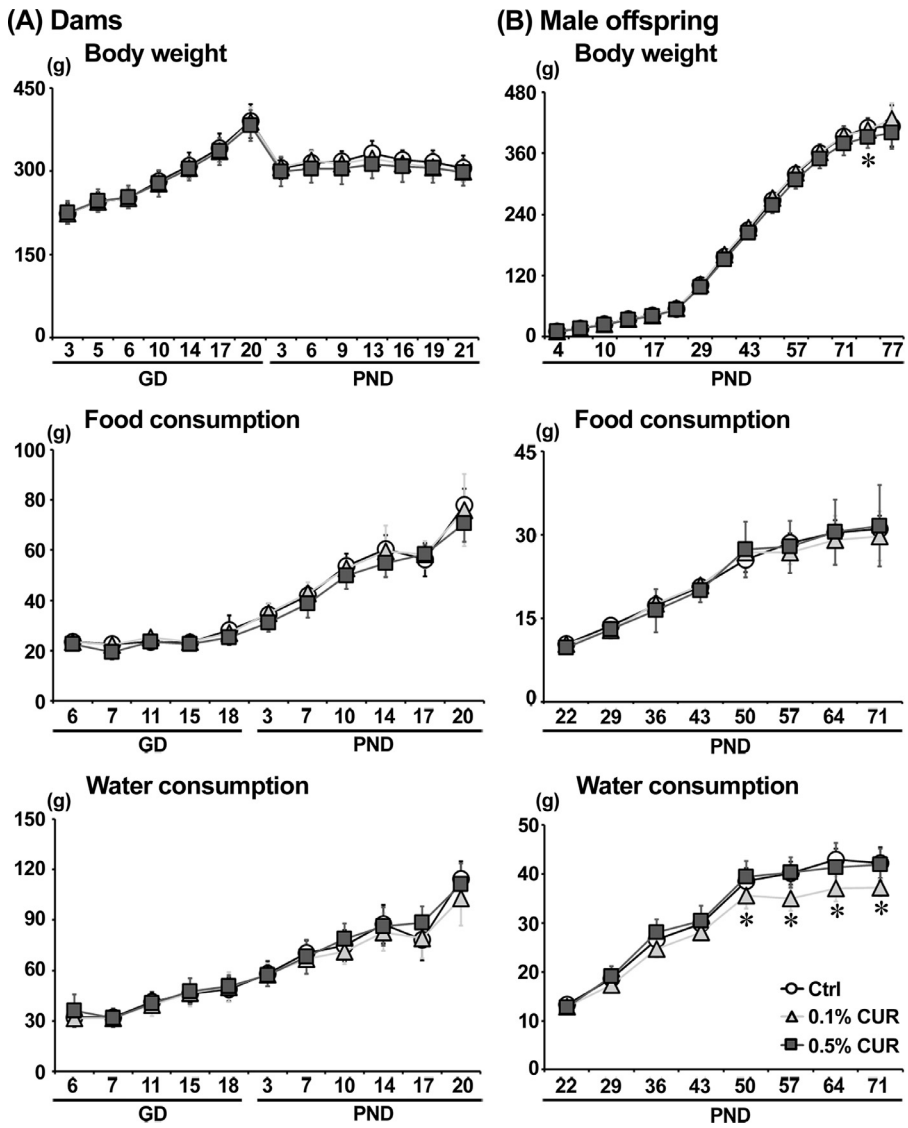

Fig. 5 – Body weight, food and water consumption of dams and offspring during experiment. (A) Dams. (B) Male offspring. Values are expressed as means ± SD. *P < .05, compared with the vehicle controls by Dunnett's test or Aspin–Welch's t test with Bonferroni correction.

neous data, Aspin–Welch's *t*-test with Bonferroni correction was used. These analyses were performed using IBM SPSS Statistics ver. 25 (International Business Machines Corporation, Armonk, NY, USA), and $P < 0.05$ was considered statistically significant.

3. Results

3.1. *Maternal parameters*

In the vehicle controls and 0.1% CUR, one each of nonpregnant animal was excluded from the experiment. One pregnant animal each of the vehicle controls and 0.5% CUR was used for measurement of curcumin concentrations in the gastric milk content of offspring. Therefore, the effective numbers of dams were 12, 12, and 13 for the vehicle controls, 0.1% CUR, and 0.5% CUR, respectively. Dams in each exposure group showed no significant changes in BW and in food and water consumption during gestation and lactation periods compared with the vehicle controls (Fig. 5A).

Based on the mean food consumption values, dams in the 0.1% CUR and 0.5% CUR received 85.8 and 398.9 mg/kg BW/day curcumin, respectively, during the gestation period. Dams consumed 172.3 and 825.8 mg/kg BW/day curcumin during the lactation period, respectively.

3.2. *Curcumin concentration in the plasma and gastric content of offspring*

Curcumin concentrations in the plasma content of male offspring at PND 21 were below the detection limit (0.1 μg/mL) in the vehicle controls and 2.78 μg/mL in the 0.5% CUR.

Curcumin concentrations in the gastric milk content of female offspring at PND 14 were below the detection limit (1.0 μg/g) in the vehicle controls and 25.6 μg/g in the 0.5% CUR.

3.3. *In life parameter data and necropsy data in offspring*

No changes in the gait and behaviors were observed in offspring of any exposure group before necropsy on PND 21 and after weaning, but yellow dyeing of the fur and soft stools were observed in the 0.5% CUR animals. BW of male offspring of the 0.5% CUR significantly decreased on PND 71 compared to the vehicle controls ($P < .05$ by Dunnett's test or Aspin–Welch's *t*-test with Bonferroni correction; Fig. 5B). There were no significant differences in food consumption in any exposure group. Water consumption was significantly decreased from PND 50 to PND 71 only in the 0.1% CUR compared with the vehicle controls ($P < .05$ by Dunnett's test or Aspin–Welch's *t*-test with Bonferroni correction).

Based on the mean food consumption values after weaning, offspring in the 0.1% CUR and 0.5% CUR received 106.4 and 556.0 mg/kg BW/day curcumin, respectively.

3.4. *Behavioral testing scores in male offspring*

3.4.1. *OFT*

Animals in the 0.1% CUR showed significantly higher center region time compared with the vehicle controls ($P < .01$ by Dunnett's test or Aspin–Welch's *t*-test with Bonferroni correction), while the 0.5% CUR did not differ from the vehicle controls (Fig. 6A, Table 4). There were no significant differences in activity scores (total distance and total movement duration) between the vehicle controls and each exposure group.

3.4.2. *OLT and ORT*

In both tests, the discrimination index in the test phase after a 24 hours interval showed no significantly different memory performance in any exposure group, as the discrimination index was about 0.5 or less (Table 4).

3.4.3. *Contextual fear conditioning test*

Because there was a certain number of poor learners on contextual fear conditioning, an outlier test was performed and 5 outliers out of 24 animals in the 0.1% CUR and 3 outliers out of 26 animals in the 0.5% CUR were identified, respectively (Table 4).

There were no significant differences in the freezing time in the fear-acquisition test at 24 hours after fear conditioning between the vehicle controls and each exposure group (Fig. 6B, Table 4). Regarding the freezing time in the fear-extinction test, the 0.1% CUR showed a significantly lower rate at the 2nd and 3rd trials compared with the vehicle controls ($P < .05$ by Dunnett's test or Aspin–Welch's *t*-test with Bonferroni correction), while the 0.5% CUR did not differ from that of the vehicle controls.

3.5. *Immunohistochemical results in male offspring*

3.5.1. *Synaptic plasticity-related molecule$^+$ cells after the last trial of fear-extinction test*

In the hippocampal GCL, the 0.1% CUR showed a significantly higher number of FOS$^+$ and ARC$^+$ cells compared with the vehicle controls ($P < .05$ by Dunnett's test or Aspin–Welch's *t*-test with Bonferroni correction), while the 0.5% CUR did not differ significantly from the vehicle controls (Fig. 7A, Table 5). There were no significant differences in the number of COX2$^+$, EGR1$^+$, and p-ERK1/2$^+$ cells in the GCL between the vehicle controls and each exposure group.

In the prelimbic cortex of the mPFC, the 0.1% CUR showed a significantly lower number of p-ERK1/2$^+$ cells compared with the vehicle controls ($P < .05$ by Dunnett's test or Aspin–Welch's *t*-test with Bonferroni correction), while the number of p-ERK1/2$^+$ cells in the 0.5% CUR did not differ significantly from the vehicle controls (Fig. 7A, Table 5). There were no significant differences in the number of FOS$^+$, ARC$^+$, and COX2$^+$ cells between the vehicle controls and each exposure group.

In the infralimbic cortex of the mPFC, there were no significant differences in the number of FOS$^+$, ARC$^+$, COX2$^+$, and p-ERK1/2$^+$ cells between the vehicle controls and each exposure group (Table 5).

3.5.2. *Neurogenesis-related cell populations and glial cells in the hippocampal dentate gyrus of animals not used for behavioral studies*

Regarding granule cell lineage subpopulations, the 0.5% CUR showed a significantly higher number of GFAP$^+$ cells in the SGZ compared with the vehicle controls ($P < .05$ by Dunnett's test or Aspin–Welch's *t*-test with Bonferroni correction), while the 0.1% CUR did not differ from the vehicle controls (Fig. 7B, Table 6). There were no significant differences in the number of SOX2$^+$ and TBR2$^+$ cells in the SGZ, and DCX$^+$, TUBB3$^+$, and NeuN$^+$ cells in the SGZ and GCL between the vehicle controls and each exposure group. Regarding the PCNA$^+$ proliferating cells in the SGZ, the 0.5% CUR showed a significantly higher number compared with the vehicle controls ($P < .05$ by Dunnett's test or Aspin–Welch's *t*-test with Bonferroni correction), while PCNA$^+$ cells in the 0.1% CUR did not differ statistically from the vehicle controls. There were no significant differences in the number of TUNEL$^+$ apoptotic cells in the SGZ between the vehicle controls and each exposure group. Regarding synaptic plasticity-related molecule-immunoreactive cells in the GCL, there were no significant differences in the number of FOS$^+$ and ARC$^+$ cells between the vehicle controls and each exposure group. There were no significant differences in the densities of PVALB$^+$, CALB2$^+$, and SST$^+$ interneurons, GFAP$^+$ astrocytes, and IBA1$^+$ microglia in the hilus of the dentate gyrus between the vehicle controls and each exposure group.

3.6. *Transcript-level expression in male offspring*

3.6.1. *Hippocampal dentate gyrus*

In the 0.1% CUR, the transcript levels of *Grin2d, Slc17a6, Fos,* and *Calb2* were significantly increased ($P < .01$ with *Grin2d, Slc17a6,* and *Fos; P* < .01 or 0.05 with *Calb2* by Dunnett's test or Aspin–Welch's *t*-test with Bonferroni correction), while the transcript levels of *Gria1, Gria2, Slc17a7, Arc, Ptgs2,* and *Sst* were significantly decreased ($P < .01$ or .05 with *Arc* and *Sst; P* < .05 with *Gria1, Gria2, Slc17a7,* and *Ptgs2* by Dunnett's test or Aspin–Welch's *t*-test with Bonferroni correction) after normalization with *Gapdh* and *Hprt1* compared with the levels in the vehicle controls (Table 7).

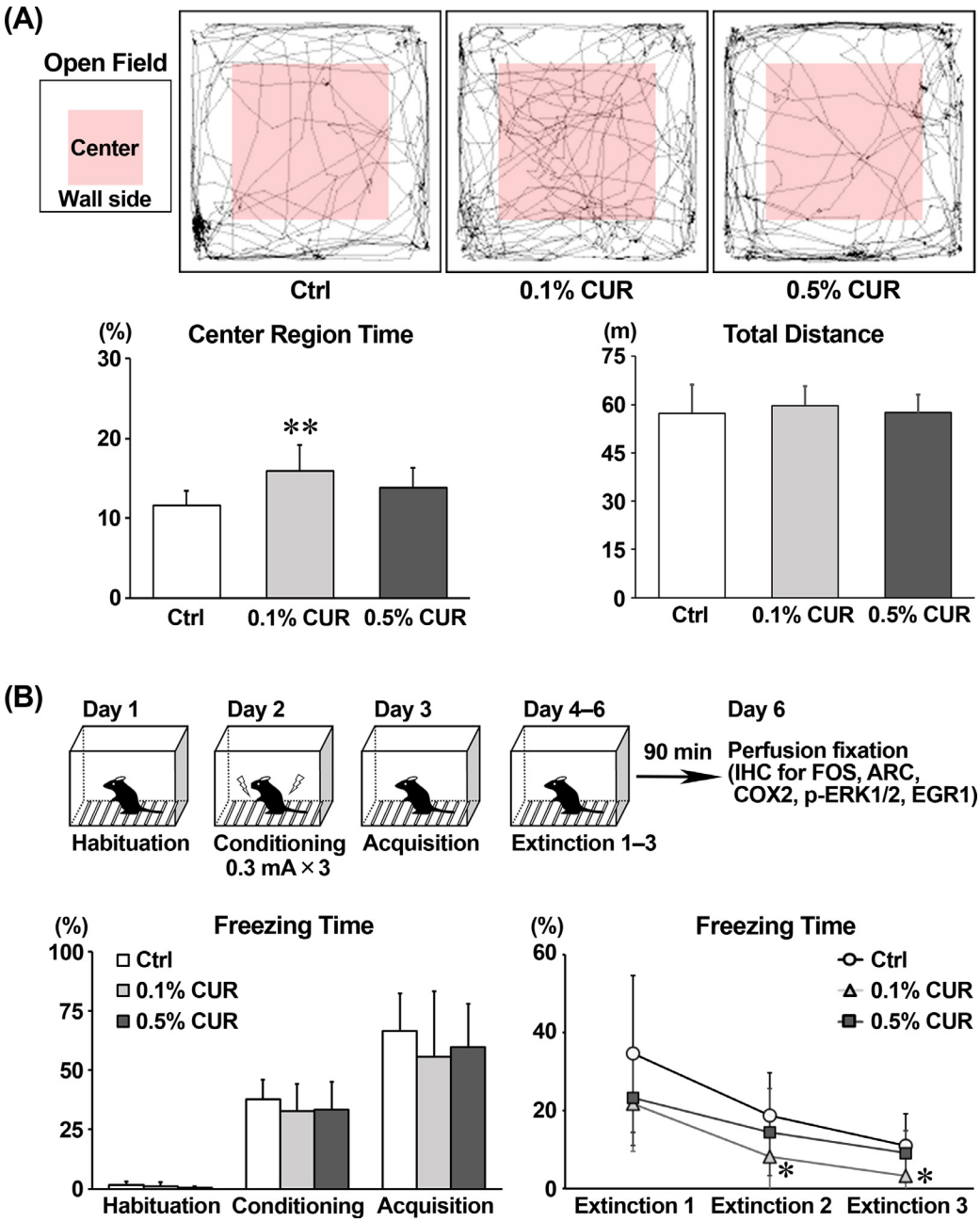

Fig. 6 – Behavioral tests. (A) Open field test. Upper panel shows representative examples of animal track in each group. Graphs show the percent of time in the center region and total distance traveled. N = 24 to 26 in each group (2 animals per dam). (B) Contextual fear conditioning test. Upper panel shows experimental design. Graphs show the rate of the freezing time in the habituation, fear conditioning, fear acquisition and fear extinction. N = 24 to 26 in each group (2 animals per dam; 5 and 3 animals that were detected as fear-extinction outliers by the Smirnov-Grubbs test were excluded from data analysis in the 0.1% CUR and 0.5% CUR, respectively). Values are expressed as means + SD or means ± SD. *P < .05, **P < .01, compared with the vehicle controls by Dunnett's test or Aspin–Welch's t test with Bonferroni correction.

In the 0.5% CUR, the transcript levels of *Gria3*, *Grin2b*, *Grin2c*, *Fos*, *Keap1*, *Nos2*, *Nos3*, *Nfkb1*, *Il4*, *Il6*, and *Tnf* were significantly increased ($P < .01$ with *Grin2c*, *Keap1*, *Nos3*, *Nfkb1*, and *Il4*; $P < .01$ or .05 with *Grin2b*, *Nos2*, and *Tnf*; $P < .05$ with *Gria3*, *Fos*, and *Il6* by Dunnett's test or Aspin–Welch's *t*-test with Bonferroni correction) after normalization with *Gapdh* and/or *Hprt1* compared with the levels in the vehicle controls (Table 7).

3.6.2. *Amygdala*

In the 0.1% CUR, the transcript levels of *Gria1*, *Gria2*, *Grin2d*, and *Slc17a6* were significantly increased ($P < .01$ or .05 with

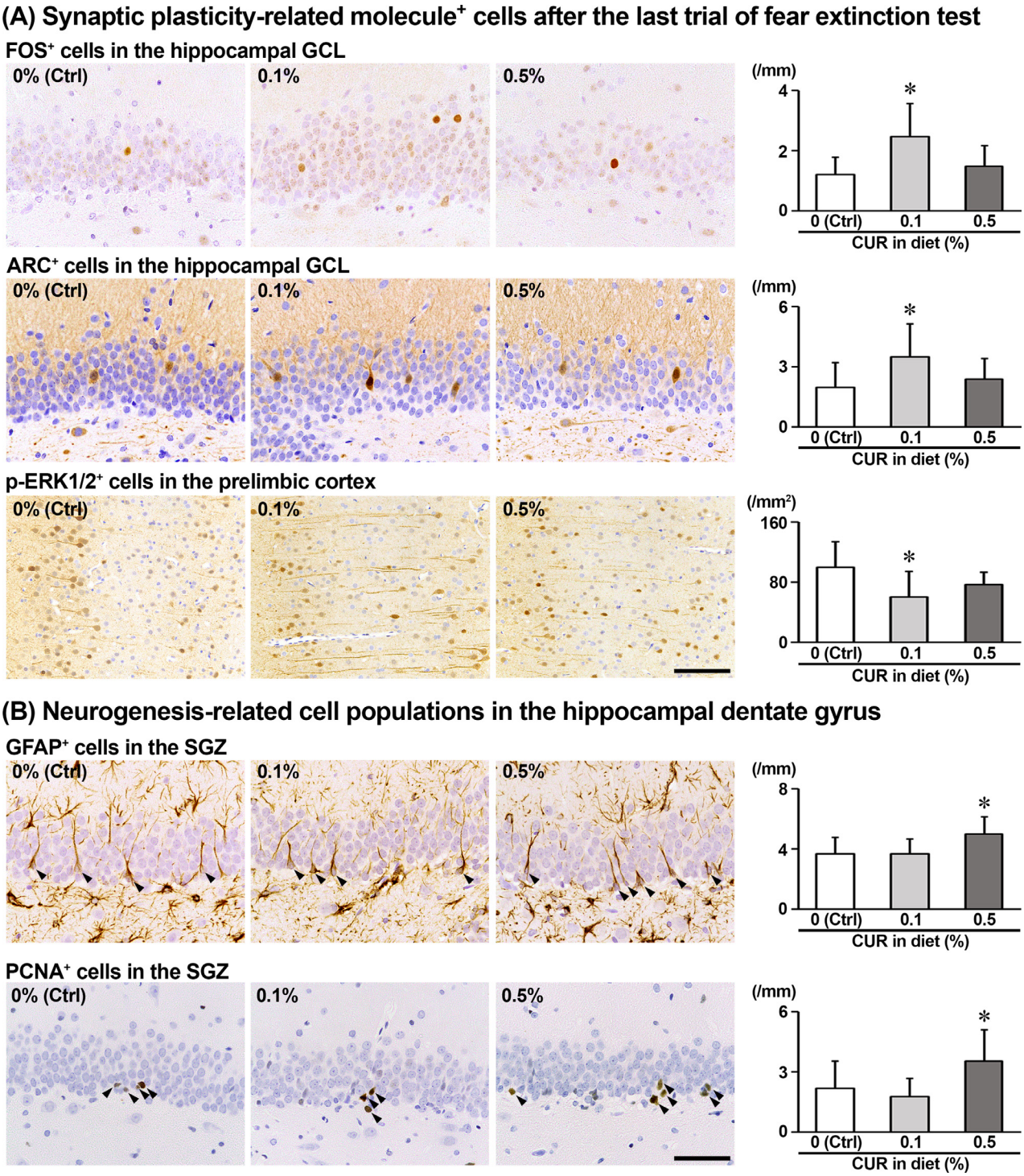

Fig. 7 – Representative immunohistochemistry results. (A) The number of immunoreactive cells for synaptic plasticity-related molecules in the hippocampal GCL and the prelimbic cortex after the last trial of fear-extinction test. Representative images from the vehicle controls (left), 0.1% CUR group (middle) and 0.5% CUR group (right) on PND 74. Magnification × 400; bar = 50 μm. The graphs show the number of immunoreactive cells/unit length (mm) of the SGZ of the bilateral sides or the number of immunoreactive cells/unit area (mm^2) in the prelimbic cortex of the bilateral sides. Values are expressed as means + SD. N = 9 to 10 in each group (1 animal per dam). (B) The number of neurogenesis-related cell populations in the hippocampal dentate gyrus of animals that were not subjected to behavioral tests. Representative images from the vehicle controls (left), 0.1% CUR group (middle) and 0.5% CUR group (right) on PND 77. Arrowheads indicate immunoreactive cells. Magnification × 400; bar 50 µm. The graphs show the number of immunoreactive cells/unit length (mm) of the SGZ of the bilateral sides. Values are expressed as means + SD. N = 10 in each group (1 animal per dam). *P < .05, compared with the vehicle controls by Dunnett's test or Aspin–Welch's t test with Bonferroni correction.

Table 4 – Changes in the behavioral tests in male offspring

		Ctrl	0.1% CUR	0.5% CUR
Open field test				
No. of offspring examined (2 pups/dam)		24	24	26
Total distance (cm)		5737.2 ± 887.1[a]	5972.9 ± 606.6	5744.5 ± 564.3
Total movement duration (s)		288.7 ± 33.9	304.6 ± 27.4	291.0 ± 22.5
Wall side time (s)		530.8 ± 11.6	504.2 ± 19.0**	517.3 ± 14.8
Center region time (s)		69.2 ± 11.6	95.8 ± 19.0**	82.8 ± 14.8
Object location test				
No. of offspring examined (1 pup/dam)		12	12	13
Total distance (cm)				
Sample phase		3599.8 ± 529.0	3688.7 ± 460.4	3578.6 ± 306.1
Test phase		2205.5 ± 315.4	2446.1 ± 315.9	2302.6 ± 314.3
Discrimination index				
Sample phase		0.47 ± 0.15	0.49 ± 0.08	0.51 ± 0.14
Test phase		0.52 ± 0.12	0.48 ± 0.17	0.43 ± 0.15
Object recognition test				
No. of offspring examined (1 pup/dam)		12	12	13
Total distance (cm)				
Sample phase		3569.0 ± 390.1	3799.0 ± 400.6	3577.6 ± 388.0
Test phase		2216.6 ± 303.3	2431.4 ± 321.6	2386.8 ± 149.6
Discrimination index				
Sample phase		0.48 ± 0.11	0.42 ± 0.13	0.44 ± 0.07
Test phase		0.54 ± 0.11	0.49 ± 0.10	0.50 ± 0.11
Contextual fear conditioning test				
No. of offspring examined (1-2 pups/dam)		24	24 (19)[b]	26 (23)[c]
Freezing time (%)				
Day 1	Habituation	1.7 ± 1.5	1.2 ± 1.6	0.5 ± 0.7
Day 2	Fear conditioning	37.7 ± 8.3	32.8 ± 11.4	33.3 ± 11.6
Day 3	Fear acquisition	66.4 ± 15.9	55.6 ± 27.6	59.6 ± 18.4
Day 4	Fear extinction 1	34.5 ± 20.1	21.7 ± 14.5	23.2 ± 12.1
Day 5	Fear extinction 2	18.6 ± 11.1	8.1 ± 3.6*	14.5 ± 11.2
Day 6	Fear extinction 3	10.9 ± 8.2	3.3 ± 1.5*	9.15 ± 5.8

Abbreviations: Ctrl, vehicle controls; CUR, amorphous formula of curcumin.
[a] Means ± SD.
[b] Five animals that were detected as fear-extinction outliers by the Smirnov-Grubbs test were excluded from data analysis. The number in parenthesis is the effective number of animals.
[c] Three animals that were detected as fear-extinction outliers by the Smirnov-Grubbs test were excluded from data analysis. The number in parenthesis is the effective number of animals.*$P < .05$, **$P < .01$, compared with the vehicle controls by Dunnett's test or Aspin–Welch's *t*-test with Bonferroni correction.

Grin2d; $P < .05$ with *Gria1*, *Gria2*, and *Slc17a6* by Dunnett's test or Aspin–Welch's *t*-test with Bonferroni correction) after normalization with *Gapdh* and/or *Hprt1* compared with the levels in the vehicle controls (Table 8).

In the 0.5% CUR, the transcript level of *Grin2d* was significantly increased ($P < .05$ by Dunnett's test or Aspin–Welch's *t*-test with Bonferroni correction) after normalization with *Gapdh* and *Hprt1* compared with the levels in the vehicle controls (Table 8).

3.6.3. *mPFC*

In the 0.1% CUR, the transcript levels of *Gria1*, *Grin2c*, and *Slc17a6* were significantly increased ($P < .01$ with *Gria1* and *Grin2c*; $P < .05$ with *Slc17a6* by Dunnett's test or Aspin–Welch's *t*-test with Bonferroni correction) in the prelimbic cortex, while the transcript level of *Grin2a* was significantly decreased ($P < .05$ by Dunnett's test or Aspin–Welch's *t*-test with Bonferroni correction) in this region after normalization with *Gapdh* or *Hprt1* compared with the levels in the vehicle controls (Table 8). In the infralimbic cortex, the transcript level of *Slc17a6* was significantly increased ($P < .01$ by Dunnett's test or Aspin–Welch's *t*-test with Bonferroni correction), while the transcript levels of *Grin2a*, *Grin2b*, *Grin2d*, and *Slc17a7* were significantly decreased ($P < .05$ with *Grin2a*, *Grin2b*, *Grin2d*, and *Slc17a7* by Dunnett's test or Aspin–Welch's *t*-test with Bonferroni correction) after normalization with *Gapdh* and/or *Hprt1* compared with the levels in the vehicle controls. In the 0.5% CUR, the transcript level of *Gria1* was significantly increased ($P < .05$ by Dunnett's test or Aspin–Welch's *t*-test with Bonferroni correction) in the prelimbic cortex after normalization with *Gapdh* and *Hprt1* compared with the levels in the vehicle controls (Table 8). In the infralimbic cortex, there were no genes encoding glutamate receptors and transporters to change the transcript level compared with the levels in the vehicle controls.

4. Discussion

We recently found that continued exposure to α-glycosyl isoquercitrin (AGIQ), a polyphenolic flavonol glycoside derived by enzymatic glycosylation of rutin, from developmental

Table 5 – Number of immunoreactive cells for synaptic plasticity-related molecules after the last trial of fear extinction test in male offspring

	Ctrl	0.1% CUR	0.5% CUR
Hippocampal GCL (No./mm SGZ length)			
No. of animals examined	10	10	10
FOS	1.21 ± 0.57[a]	2.47 ± 1.10*	1.50 ± 0.68
ARC	1.98 ± 1.23	3.50 ± 1.64*	2.40 ± 1.04
COX2	6.26 ± 2.03	7.43 ± 3.27	5.76 ± 2.80
EGR1	9.19 ± 3.09	9.05 ± 4.19	8.56 ± 3.76
p-ERK1/2	3.47 ± 1.27	3.84 ± 1.95	3.44 ± 1.41
Prelimbic cortex (No./mm^2 measured area)			
No. of animals examined	10	9	10
FOS	13.49 ± 6.89	17.29 ± 8.66	17.26 ± 8.26
ARC	75.40 ± 38.75	90.73 ± 32.13	74.60 ± 25.80
COX2	10.69 ± 6.79	14.03 ± 12.04	15.81 ± 13.03
p-ERK1/2	100.68 ± 33.16	60.33 ± 34.10*	77.20 ± 16.46
Infralimbic cortex (No./mm^2 measured area)			
No. of animals examined	9	9	10
FOS	9.35 ± 3.01	18.01 ± 8.59	15.93 ± 10.03
ARC	42.98 ± 18.06	58.21 ± 38.89	33.37 ± 17.73
COX2	7.96 ± 4.71	11.24 ± 6.47	14.54 ± 11.15
p-ERK1/2	138.31 ± 51.04	119.17 ± 41.42	136.23 ± 17.14

Abbreviations: ARC, activity-regulated cytoskeleton-associated protein; COX2, cyclooxygenase-2; Ctrl, vehicle control; CUR, amorphous formula of curcumin; FOS, Fos proto-oncogene, AP-1 transcription factor subunit; GCL, granule cell layer; EGR1, early growth response protein 1; p-ERK1/2, phosphorylated extracellular signal-regulated kinase 1/2 (phosphorylated p44/p42 MAP kinase); SGZ, subgranular zone.

[a] Means ± SD.

* $P < .05$, compared with the vehicle controls by Dunnett's test or Aspin–Welch's *t* test with Bonferroni correction.

Table 6 – Number of immunoreactive cells in the SGZ/GCL and hilar region of the hippocampal dentate gyrus of male offspring not subjected to behavioral tests

	Ctrl	0.1% CUR	0.5% CUR
No. of animals examined	10	10	10
Granule cell lineage subpopulations (No./mm SGZ length)			
GFAP	3.70 ± 1.08[a]	3.71 ± 0.97	5.02 ± 1.13*
SOX2	14.17 ± 3.43	15.30 ± 4.51	13.73 ± 4.91
TBR2	2.56 ± 1.76	2.75 ± 1.98	3.34 ± 1.90
DCX	8.91 ± 3.65	11.94 ± 4.13	9.80 ± 3.37
TUBB3	2.28 ± 1.67	3.41 ± 2.71	4.48 ± 3.00
NeuN	521.04 ± 42.24	552.84 ± 57.37	505.89 ± 52.88
Cell proliferation and apoptosis (No./mm SGZ length)			
PCNA	2.20 ± 1.34	1.77 ± 0.91	3.56 ± 1.54*
TUNEL	0.18 ± 0.20	0.07 ± 0.11	0.16 ± 0.22
Synaptic plasticity-related molecules (No./mm SGZ length)			
FOS	1.03 ± 0.40	1.02 ± 0.41	1.11 ± 0.64
ARC	2.66 ± 1.09	3.44 ± 1.54	2.17 ± 1.04
Interneuron subpopulations (No./mm^2 hilar region)			
PVALB	17.41 ± 4.43	19.58 ± 5.16	23.83 ± 10.71
CALB2	1.37 ± 1.38	0.82 ± 1.11	1.43 ± 1.15
SST	33.94 ± 15.32	36.04 ± 12.10	24.10 ± 10.83
Astrocytes and microglia (No./mm^2 hilar region)			
GFAP	191.03 ± 23.55	179.85 ± 23.72	194.65 ± 29.39
IBA1	100.94 ± 20.51	88.95 ± 11.04	115.23 ± 24.36

Abbreviations: ARC, activity-regulated cytoskeleton-associated protein; CALB2, calbindin-D-29 K; Ctrl, vehicle control; CUR, amorphous formula of curcumin; DCX, doublecortin; FOS, Fos proto-oncogene, AP-1 transcription factor subunit; GCL, granule cell layer; GFAP, glial fibrillary acidic protein; IBA1, ionized calcium-binding adaptor molecule 1; NeuN, neuronal nuclei; PCNA, proliferating cell nuclear antigen; PVALB, parvalbumin; SGZ, subgranular zone; SOX2, SRY-box transcription factor 2; SST, somatostatin; TBR2, T-box brain protein 2; TUBB3, tubulin, beta 3 class III; TUNEL, terminal deoxynucleotidyl transferase-mediated dUTP-biotin nick end-labeling.

[a] Means ± SD.

* $P < .05$, compared with the vehicle controls by Dunnett's test or Aspin–Welch's *t* test with Bonferroni correction.

Table 7 – Transcript level expression changes in the hippocampal dentate gyrus of male offspring not subjected to behavioral tests

	Ctrl		0.1% CUR		0.5% CUR	
Normalization control	*Gapdh*	*Hprt1*	*Gapdh*	*Hprt1*	*Gapdh*	*Hprt1*
No. of animals examined	6	6	6	6	6	6
Glutamate receptors						
Gria1	1.08 ± 0.45[a]	1.07 ± 0.41	0.40 ± 0.16*	0.40 ± 0.18*	1.10 ± 0.65	1.14 ± 0.60
Gria2	1.06 ± 0.41	1.06 ± 0.36	0.45 ± 0.15*	0.45 ± 0.17*	1.11 ± 0.62	1.15 ± 0.51
Gria3	1.03 ± 0.27	1.03 ± 0.25	0.85 ± 0.15	0.86 ± 0.22	1.26 ± 0.37	1.36 ± 0.18*
Grin2a	1.06 ± 0.37	1.05 ± 0.33	0.72 ± 0.17	0.72 ± 0.21	1.37 ± 0.61	1.45 ± 0.50
Grin2b	1.04 ± 0.33	1.05 ± 0.31	1.09 ± 0.14	1.11 ± 0.27	1.45 ± 0.19*	1.61 ± 0.18**
Grin2c	1.03 ± 0.26	1.02 ± 0.20	1.42 ± 0.16	1.43 ± 0.27	2.02 ± 0.56**	2.35 ± 1.16**
Grin2d	1.03 ± 0.28	1.04 ± 0.30	2.17 ± 0.43**	2.17 ± 0.44**	1.41 ± 0.57	1.62 ± 0.87
Glutamate transporters						
Slc17a6	1.16 ± 0.58	1.18 ± 0.65	4.09 ± 1.33**	4.04 ± 1.18**	1.52 ± 0.75	1.80 ± 1.17
Slc17a7	1.03 ± 0.25	1.02 ± 0.24	0.58 ± 0.25*	0.58 ± 0.24*	0.82 ± 0.38	0.87 ± 0.36
Synaptic plasticity-related genes						
Fos	1.06 ± 0.36	1.08 ± 0.46	2.76 ± 0.84**	2.73 ± 0.75**	2.11 ± 0.67*	2.46 ± 1.15*
Jun	1.03 ± 0.28	1.01 ± 0.19	0.84 ± 0.18	0.85 ± 0.26	0.90 ± 0.26	0.98 ± 0.20
Arc	1.05 ± 0.37	1.04 ± 0.29	0.50 ± 0.19*	0.50 ± 0.17**	1.06 ± 0.40	1.13 ± 0.31
Ptgs2	1.08 ± 0.44	1.07 ± 0.40	0.38 ± 0.25*	0.39 ± 0.25*	0.87 ± 0.51	0.90 ± 0.45
Egr1	1.02 ± 0.21	1.04 ± 0.31	1.08 ± 0.23	1.08 ± 0.23	1.25 ± 0.23	1.37 ± 0.16
Oxidative stress-related genes						
Nfe2l2	1.05 ± 0.39	1.03 ± 0.27	1.00 ± 0.14	1.03 ± 0.29	0.97 ± 0.05	1.09 ± 0.22
Keap1	1.01 ± 0.18	1.02 ± 0.22	1.26 ± 0.36	1.31 ± 0.40	2.00 ± 0.36**	1.25 ± 0.20
Nos1	1.18 ± 0.71	1.16 ± 0.68	0.65 ± 0.21	0.66 ± 0.27	1.32 ± 0.66	1.39 ± 0.56
Nos2	1.31 ± 0.97	1.48 ± 1.28	4.47 ± 2.63	4.59 ± 2.88	37.80 ± 15.52**	43.93 ± 26.96*
Nos3	1.05 ± 0.33	1.03 ± 0.26	1.41 ± 0.30	1.44 ± 0.49	2.50 ± 0.47**	2.85 ± 0.99**
Chemical mediators and related molecules						
Nfkb1	1.06 ± 0.42	1.02 ± 0.21	1.22 ± 0.57	1.22 ± 0.42	2.00 ± 0.41**	1.26 ± 0.29
Il1a	1.13 ± 0.63[b]	1.05 ± 0.34	1.11 ± 0.66	1.03 ± 0.76	1.49 ± 0.83	0.99 ± 0.49
Il1b	1.12 ± 0.62[b]	1.05 ± 0.36	0.84 ± 0.59	0.74 ± 0.59	1.10 ± 0.21	0.75 ± 0.12
Il4	1.10 ± 0.53[b]	1.03 ± 0.26	1.10 ± 0.43	0.98 ± 0.33	2.64 ± 0.52**	1.82 ± 0.41**
Il6	1.47 ± 1.28[b]	1.41 ± 1.04	2.28 ± 1.29	1.99 ± 0.96	3.38 ± 1.46*	2.32 ± 1.08
Tnf	1.32 ± 0.95	1.22 ± 0.64	1.28 ± 1.36	1.14 ± 0.83	14.81 ± 6.47**	9.39 ± 4.60*
Interneuron marker genes						
Pvalb	1.40 ± 1.57	1.23 ± 1.01	0.93 ± 0.37	0.98 ± 0.43	1.25 ± 0.71	0.79 ± 0.51
Calb2	1.07 ± 0.39	1.07 ± 0.44	2.22 ± 0.65*	2.22 ± 0.56**	1.21 ± 0.92	1.28 ± 0.76
Sst	1.06 ± 0.36	1.02 ± 0.23	0.40 ± 0.19*	0.41 ± 0.20**	0.69 ± 0.48	0.69 ± 0.39
Reln	1.08 ± 0.44	1.03 ± 0.26	0.89 ± 0.23	0.91 ± 0.30	0.86 ± 0.39	0.91 ± 0.23

Abbreviations: *Arc*, activity-regulated cytoskeleton-associated protein; *Calb2*, calbindin 2 (also known as calbindin-D-29K); Ctrl, vehicle control; CUR, amorphous formula of curcumin; *Egr1*, early growth response protein 1; *Fos*, Fos proto-oncogene, AP-1 transcription factor subunit; *Gapdh*, glyceraldehyde-3-phosphate dehydrogenase; *Gria1*, glutamate ionotropic receptor AMPA type subunit 1; *Gria2*, glutamate ionotropic receptor AMPA type subunit 2; *Gria3*, glutamate ionotropic receptor AMPA type subunit 3; *Grin2a*, glutamate ionotropic receptor NMDA type subunit 2A; *Grin2b*, glutamate ionotropic receptor NMDA type subunit 2B; *Grin2c*, glutamate ionotropic receptor NMDA type subunit 2C; *Grin2d*, glutamate ionotropic receptor NMDA type subunit 2D; *Hprt1*, hypoxanthine phosphoribosyltransferase 1; *Il1a*, interleukin 1 alpha; *Il1b*, interleukin 1 beta; *Il4*, interleukin 4; *Il6*, interleukin 6; *Jun*, Jun proto-oncogene, AP-1 transcription factor subunit; *Keap1*, Kelch-like ECH-associated protein 1; *Nfe2l2*, nuclear factor, erythroid 2-like 2; *Nfkb1*, nuclear factor kappa B subunit 1; *Nos1*, nitric oxide synthase 1; *Nos2*, nitric oxide synthase 2; *Nos3*, nitric oxide synthase 3; *Ptgs2*, prostaglandin-endoperoxide synthase 2; *Pvalb*, parvalbumin; *Reln*, reelin; *Slc17a6*, solute carrier family 17 member 6; *Slc17a7*, solute carrier family 17 member 7; *Sst*, somatostatin; *Tnf*, tumor necrosis factor.

[a] Means ± SD.

[b] Values were obtained from animals that were subjected to behavioral tests.*$P < .05$, **$P < .01$, compared with the vehicle controls by Dunnett's test or Aspin–Welch's *t* test with Bonferroni correction.

stage facilitated fear-extinction learning and upregulated the constitutive expression level of *Fos* in the hippocampal dentate gyrus and *Grin2d* in the amygdala [28]. In the present study, we tested CUR that has enabled an improved bioavailability after oral intake and found that exposure of rats to 0.1% CUR led to an increase in the time spent in the center region of the open field test device without changing motor activity in an OFT, suggesting an antianxiety-like effect, and facilitation of fear-extinction learning in the contextual fear conditioning test. However, there were no changes in the OLT or the ORT that evaluated spatial and nonspatial memory. Regarding the changes in the constitutive gene expression level, 0.1% CUR upregulated *Fos* in the hippocampal dentate gyrus and glutamate receptors, represented by *Grin2d* in the dentate gyrus and amygdala. While we did not perform OFT in our previous AGIQ study, these results

Table 8 – Transcript level expression changes of glutamate receptors and transporters in the amygdala, prelimbic cortex and infralimbic cortex of male offspring not subjected to behavioral tests

	Ctrl		0.1% CUR		0.5% CUR	
Normalization control	*Gapdh*	*Hprt1*	*Gapdh*	*Hprt1*	*Gapdh*	*Hprt1*
No. of animals examined	6	6	6	6	6	6
Amygdala						
Gria1	1.01 ± 0.13[a]	1.01 ± 0.12	1.29 ± 0.15*	1.19 ± 0.22	1.20 ± 0.26	1.14 ± 0.28
Gria2	1.01 ± 0.13	1.00 ± 0.10	1.18 ± 0.11*	1.08 ± 0.16	1.15 ± 0.08	1.09 ± 0.11
Gria3	1.03 ± 0.25	1.01 ± 0.18	1.14 ± 0.12	1.05 ± 0.18	1.15 ± 0.11	1.08 ± 0.11
Grin2a	1.01 ± 0.18	1.01 ± 0.13	1.08 ± 0.16	1.00 ± 0.23	1.16 ± 0.16	1.10 ± 0.20
Grin2b	1.01 ± 0.16	1.01 ± 0.12	1.10 ± 0.10	1.02 ± 0.17	1.15 ± 0.07	1.09 ± 0.10
Grin2c	1.01 ± 0.17	1.01 ± 0.16	1.02 ± 0.08	0.94 ± 0.13	1.01 ± 0.11	0.96 ± 0.13
Grin2d	1.04 ± 0.30	1.04 ± 0.33	2.22 ± 0.47**	2.02 ± 0.38*	2.06 ± 0.86*	1.95 ± 0.83*
Slc17a6	1.02 ± 0.23	1.02 ± 0.23	1.40 ± 0.19*	1.28 ± 0.22	1.29 ± 0.31	1.23 ± 0.34
Slc17a7	1.04 ± 0.28	1.02 ± 0.22	1.06 ± 0.24	0.99 ± 0.31	1.30 ± 0.27	1.23 ± 0.26
Prelimbic cortex						
Gria1	1.02 ± 0.24	1.00 ± 0.06	1.00 ± 0.30	1.21 ± 0.12**	1.45 ± 0.20*	1.18 ± 0.12*
Gria2	1.03 ± 0.24	1.00 ± 0.07	0.81 ± 0.16	1.01 ± 0.13	1.26 ± 0.23	1.02 ± 0.15
Gria3	1.03 ± 0.25	1.00 ± 0.09	0.79 ± 0.18	0.99 ± 0.14	1.14 ± 0.23	0.94 ± 0.24
Grin2a	1.03 ± 0.25	1.01 ± 0.15	0.62 ± 0.12*	0.78 ± 0.17	1.01 ± 0.44	0.83 ± 0.37
Grin2b	1.02 ± 0.22	1.00 ± 0.07	0.82 ± 0.18	1.02 ± 0.12	1.26 ± 0.30	1.03 ± 0.26
Grin2c	1.05 ± 0.36	1.02 ± 0.21	1.22 ± 0.34	1.50 ± 0.11**	1.38 ± 0.27	1.12 ± 0.13
Grin2d	1.05 ± 0.35	1.01 ± 0.17	0.69 ± 0.21	0.84 ± 0.04	1.44 ± 0.32	1.17 ± 0.26
Slc17a6	1.03 ± 0.28	1.01 ± 0.17	1.42 ± 0.62	1.66 ± 0.33*	1.59 ± 0.63	1.29 ± 0.46
Slc17a7	1.02 ± 0.21	1.00 ± 0.07	0.78 ± 0.22	0.98 ± 0.21	1.12 ± 0.35	0.94 ± 0.34
Infralimbic cortex						
Gria1	1.02 ± 0.19	1.00 ± 0.11	1.19 ± 0.27	1.29 ± 0.25	1.39 ± 0.35	1.08 ± 0.28
Gria2	1.02 ± 0.19	1.00 ± 0.09	1.07 ± 0.23	1.17 ± 0.20	1.21 ± 0.24	0.95 ± 0.22
Gria3	1.02 ± 0.21	1.01 ± 0.15	0.98 ± 0.17	1.06 ± 0.11	1.10 ± 0.08	0.88 ± 0.23
Grin2a	1.02 ± 0.24	1.01 ± 0.13	0.74 ± 0.16*	0.80 ± 0.05*	0.94 ± 0.18	0.76 ± 0.23
Grin2b	1.02 ± 0.23	1.01 ± 0.16	0.85 ± 0.15*	0.93 ± 0.08	1.01 ± 0.12	0.80 ± 0.19
Grin2c	1.06 ± 0.37	1.03 ± 0.26	1.18 ± 0.30	1.29 ± 0.33	1.45 ± 0.49	1.14 ± 0.43
Grin2d	1.03 ± 0.27	1.02 ± 0.19	0.71 ± 0.15*	0.77 ± 0.08	1.32 ± 0.21	1.05 ± 0.27
Slc17a6	1.05 ± 0.37	1.03 ± 0.27	1.45 ± 0.31	1.57 ± 0.18**	1.65 ± 0.74	1.29 ± 0.60
Slc17a7	1.01 ± 0.16	1.00 ± 0.10	0.70 ± 0.24	0.76 ± 0.19*	0.88 ± 0.26	0.72 ± 0.29

Abbreviations: Ctrl, vehicle control; CUR, amorphous formula of curcumin; *Gapdh*, glyceraldehyde-3-phosphate dehydrogenase; *Gria1*, glutamate ionotropic receptor AMPA type subunit 1; *Gria2*, glutamate ionotropic receptor AMPA type subunit 2; *Gria3*, glutamate ionotropic receptor AMPA type subunit 3; *Grin2a*, glutamate ionotropic receptor NMDA type subunit 2A; *Grin2b*, glutamate ionotropic receptor NMDA type subunit 2B; *Grin2c*, glutamate ionotropic receptor NMDA type subunit 2C; *Grin2d*, glutamate ionotropic receptor NMDA type subunit 2D; *Hprt1*, hypoxanthine phosphoribosyltransferase 1; *Slc17a6*, solute carrier family 17 member 6; *Slc17a7*, solute carrier family 17 member 7.

[a] Means ± SD.*$P < .05$, **$P < .01$, compared with the vehicle controls by Dunnett's test or Aspin–Welch's *t* test with Bonferroni correction.

suggest that low doses of CUR may cause similar effects to AGIQ in normal animals by exposure from developmental stage.

In the present study, CUR did not show any effect on fear acquisition. In the fear-extinction test, 0.1% CUR revealed decrease in freezing time during the second and third trials of fear extinction, as compared with the vehicle controls. These results suggest that continued CUR exposure for long term from developmental stage does not alter the formation of fear memory but promotes learning of fear extinction at low dietary concentrations. Continued exposure to environmental stressors of mice results in long-term behavioral abnormality that is implicated in stress-related disorders [30]. The present study results may reinforce curcumin as an effective means of extinction-based exposure psychotherapy for prevention of stress-related disorders represented by PTSD. Interestingly, a recent study has shown that dietary treatment with 1.5% curcumin for 5 days is capable of impairing fear-memory consolidation and reconsolidation processes in rats [19]. This result suggests that curcumin may also be useful as an adjunct in the treatment of stress disorders even with brief oral treatment. Further studies may be warranted to examine the dose-effect relationship on behaviors at lower doses of CUR than those examined in the present study.

In the present study, we found a significant increase in the number of granule cells immunoreactive for FOS and ARC in the hippocampal dentate gyrus by 0.1% CUR among synaptic plasticity-related molecules 90 min after conducting the last trial of fear-extinction learning. In contrast, an increase in FOS^+ or ARC^+ cells was not confirmed at this dose in animals that had not been subjected to behavioral test, whereas constitutive expression of *Fos* was upregulated in the dentate gyrus. These results suggest an increase in synaptic plasticity mediated by FOS and ARC in association with the facilitation of fear-extinction learning. In the dentate gyrus, the expression of IEG proteins in granule cells suggested that these cells are integrated into the neural network [31]. Increased *Fos* expression in hippocampal neurons is regulated by learning-related neuronal activity [32], and mutant mice deficient in FOS in the brain show impaired spatial and contextual long-

term memory [33]. ARC also plays a critical role in the maintenance of synaptic change and in consolidation of long-term memory [13]. Moreover, 0.1% CUR exposure decreased p-ERK1/2$^+$ cells in the prelimbic cortex after the last trial of fear-extinction learning in the present study. In the mPFC, both of the prelimbic cortex and infralimbic cortex project similarly to the amygdala, and prelimbic cortex microstimulation increases conditioned fear development and inhibits extinction of fear memory, in contrast to the opposite function of the infralimbic cortex [34]. While we did not observe the alteration in the number of immunoreactive cells of any synaptic plasticity-related molecule in the infralimbic cortex, the decrease of p-ERK1/2$^+$ cells in the prelimbic cortex suggests decrease of synaptic plasticity to cause suppression of amygdala-mediated fear response that may be related to facilitation of fear-extinction learning. Thus, changes in the number of synaptic plasticity-related molecule-expressing cells in the hippocampal dentate gyrus and mPFC due to continued exposure to CUR at low doses may cause alterations in synaptic plasticity in the neural circuits involved in suppressing anxiety-like behavior and promoting fear-extinction learning.

In the present study, we examined changes in constitutive expression levels of genes encoding glutamate receptors and transporters in animals that have not been subjected to behavioral tests, and found that the glutamate receptor subunit genes were mostly expressed differently among the brain regions by 0.1% CUR exposure. Among them, *Grin2d* was strongly upregulated in the hippocampal dentate gyrus and amygdala. *Grin2d* encodes an *N*-methyl-D-aspartate (NMDA) receptor subunit and functions in enhancing the synaptic plasticity associated with long-term memory [35]. In the rat, the synaptic plasticity associated with learning and storage of both conditioned fear and fear extinction occurs within the basolateral amygdala [36]. The mechanism of memory storage in this region is thought to be long-term potentiation (LTP) by NMDA receptor activations [36]. Therefore, constitutive upregulation of *Grin2d* in the amygdala by 0.1% CUR may be involved in enhancing elimination of fear memory in the present study. In the hippocampus, the role of GRIN2D in the formation or resolution of anxiety or fear memory has not been reported until now; however, NMDA receptor hypofunction in the dentate gyrus of adult *Fmr1* knockout mice impaired extinction of contextual fear [37]. In the dentate gyrus, we also observed upregulation of *Calb2* and downregulation of *Sst* by 0.1% CUR in the present study, while the number of CALB2$^+$ or SST$^+$ GABAergic interneurons were unchanged in the hilar region. It has been reported that CALB2 expression positively contributes to the control of LTP in learning and memory in the mouse dentate gyrus by indirectly regulating the activity of GABAergic interneurons [38]. Regarding SST, while the precise role on cognitive and emotional functions is still poorly understood, one study reported that SST and the related peptide cortistatin in the dentate gyrus reduced the likelihood of generating LTP, suggestive of their role in increasing the threshold of input required for acquisition of new memories [10]. However, we did not find any influence of CUR on fear-acquisition memory. From these perspectives, altered expression of NMDA glutamate receptors and probably some interneuron proteins may be involved in suppressing anxiety or promoting fear-extinction learning.

Curcumin can attenuate oxidative stress by increasing the activity of antioxidant enzymes and activating the Nrf2-Keap1 pathway; however, the attenuating effect of oxidative stress can be abrogated and results in ROS production at high doses in cultured cells [39]. In the present study, 0.5% CUR upregulated *Keap1* transcripts in the dentate gyrus. At this dose, transcript upregulation of *Nos2* and *Nos3* was also observed in this brain region. While induction of nitric oxide synthase (NOS)−3 is sometimes neuroprotective, NOS2 induction in the brain causes detrimental oxidative damage [40]. These results suggest that 0.5% CUR causes induction of oxidative stress responses at least in the hippocampal dentate gyrus. Considering a highly bioavailable characteristics of CUR, 0.5% CUR dose may result in excess level of absorption to cause toxic effects.

Nuclear factor κB (NF-κB) is an important upstream modulator of inflammatory cytokines, and inhibition of NF-κB activation suppresses the expression of inflammatory cytokines such as interleukin (IL)−1β, IL-6, and tumor necrosis factor (TNF)-α [41]. Early neonatal exposure to TNF-α increases levels of anxiety and depression-related behaviors [42]. Therefore, *Nfkb1* transcript upregulation by 0.5% CUR in the hippocampal dentate gyrus and also in the mPFC (data not shown for the latter) in the present study might be the signature of increased production of inflammatory cytokines that cause neuroinflammation, as evidenced by transcript upregulation of *Il4*, *Il6*, and *Tnf* in the hippocampal dentate gyrus, and may inhibit the antianxiety-like effect and extinction of fear memory at this dose.

Curcumin at a low concentration promotes neurogenesis in mice and increases proliferation of cultured neural progenitor cells of mice [43]. In the present study, 0.5% CUR increased the number of GFAP$^+$ cells in the SGZ. In the hippocampus, the GFAP$^+$ SGZ cells represent type-1 neural stem cells [11]. We also observed an increase in the number of PCNA$^+$ cells in the SGZ in this group. Because the number of no other subpopulations of granule cell lineage changed, these results suggest that 0.5% CUR causes neural stem cell proliferation. Brain inflammation can cause neural stem/progenitor cells to increase in hippocampal neurogenesis, and activation of microglia plays a role in promotion of neurogenesis [44]. Microglial TNF-α is involved in nerve damage and the neurotrophic effect in hippocampal neurogenesis [23], suggesting that upregulation of *Tnf* by 0.5% CUR may contribute to the proliferation of neural stem cells.

PVP, a polymer commonly used as a stabilizer and suspending agent, was used to increase the solubility of curcumin in the present study. This chemical property may contribute to better bioavailability of curcumin and its therapeutic effect, which is consistent with our results. In the present study, 0.1% CUR showed less water consumption from PND 50 until the end of the experiment compared with the vehicle controls. The increased thirst is considered to be due to the high volume of PVP and sucrose fatty acid ester that was used as the vehicle in the vehicle controls and 0.5% CUR. There was a report that rats bred for 2 years with a diet containing 10% PVP did not show toxic effects or gross lesions [45]. Therefore, we believe that dietary concentrations of PVP in the present study are not toxic to either dams or offspring in any way that affects test results.

In conclusion, CUR at 0.1% facilitated anti-anxiety-like behavior and fear-extinction learning. The induction of synaptic plasticity-related proteins may be linked to the altered behavioral attitudes, but these changes were lacking at the 0.5% CUR concentration, probably due to induction of oxidative stress responses and neuroinflammation that affects hippocampal neurogenesis involving neural stem cells. Thus, CUR may have a better preventive effect on some stress disorders by continuous administration at low doses. In contrast, excessively absorbed doses can negate its positive effects. Further research is needed to explore the detailed mechanisms by which curcumin prevents stress disorder. The prospect of using CUR as a new effective drug for stress disorders seems promising.

CRediT authorship contribution statement

Junta Nakahara: methodology, validation, formal analysis, investigation, data curation, writing - original draft, visualization. **Yasunori Masubuchi:** investigation, writing - review and editing. **Kazumi Takashima:** investigation, writing - review & editing. **Yasunori Takahashi:** investigation, writing - review and editing. **Ryo Ichikawa:** investigation, writing - review and editing. **Tomohiro Nakao:** resources, investigation, writing - review and editing. **Mihoko Koyanagi:** resources, investigation, writing - review and editing. **Robert R Maronpot:** writing - review and editing. **Toshinori Yoshida:** writing - review and editing. **Shim-mo Hayashi:** resources, writing - review and editing, project administration. **Makoto Shibutani:** conceptualization, writing - review and editing, visualization, supervision, funding acquisition.

Acknowledgment

This work was supported by San-Ei Gen F.F.I., Inc. The authors thank Shigeko Suzuki and Yayoi Khono for their technical assistance in preparing the histological specimens. Tomohiro Nakao, Mihoko Koyanagi, and Shim-mo Hayashi are employed by food additive manufacturer whose product lines include curcumin mixed with polyvinylpyrrolidone and sucrose fatty acid ester. Robert R. Maronpot is a scientific consultant of the aforementioned food additive manufacturer. The views and opinions expressed in this article are those of the authors and not necessarily those of their respective employers. Junta Nakahara, Yasunori Masubuchi, Kazumi Takashima, Yasunori Takahashi, Ryo Ichikawa, Toshinori Yoshida, and Makoto Shibutani declare that no conflicts of interest exist.

REFERENCES

[1] Anand P, Kunnumakkara AB, Newman RA, Aggarwal BB. Bioavailability of curcumin: problems and promises. Mol Pharm 2007;4:807–18. doi:10.1021/mp700113r.

[2] Xu Y, Ku B, Cui L, Li X, Barish PA, Foster TC, et al. Curcumin reverses impaired hippocampal neurogenesis and increases serotonin receptor 1A mRNA and brain-derived neurotrophic factor expression in chronically stressed rats. Brain Res 2007;1162:9–18. doi:10.1016/j.brainres.2007.05.071.

[3] Xu Y, Ku BS, Yao HY, Lin YH, Ma X, Zhang YH, et al. Antidepressant effects of curcumin in the forced swim test and olfactory bulbectomy models of depression in rats. Pharmacol Biochem Behav 2005;82:200–6. doi:10.1016/j.pbb.2005.08.009.

[4] Ma Z, Wang N, He H, Tang X. Pharmaceutical strategies of improving oral systemic bioavailability of curcumin for clinical application. J Control Release 2019;316:359–80. doi:10.1016/j.jconrel.2019.10.053.

[5] Nakao T, Nakamura M, Nishino M Polyphenol-containing solid composition, U. S. Patent US 2018/0289635 A1. 2018-10-11, 2018.

[6] Giustino TF, Maren S. The role of the medial prefrontal cortex in the conditioning and extinction of fear. Front Behav Neurosci 2015;9:298. doi:10.3389/fnbeh.2015.00298.

[7] Adhikari A, Topiwala MA, Gordon JA. Synchronized activity between the ventral hippocampus and the medial prefrontal cortex during anxiety. Neuron 2010;65:257–69. doi:10.1016/j.neuron.2009.12.002.

[8] Amano T, Duvarci S, Popa D, Paré D. The fear circuit revisited: contributions of the basal amygdala nuclei to conditioned fear. J Neurosci 2011;31:15481–9. doi:10.1523/JNEUROSCI.3410-11.2011.

[9] Shibutani M. Hippocampal neurogenesis as a critical target of neurotoxicants contained in foods. Food Safety 2015;3:1–15. doi:10.14252/foodsafetyfscj.2014038.

[10] Tallent MK. Somatostatin in the dentate gyrus. Prog Brain Res 2007;163:265–84. doi:10.1016/S0079-6123(07)63016-7.

[11] Sibbe M, Kulik A. GABAergic regulation of adult hippocampal neurogenesis. Mol Neurobiol 2017;54:5497–510. doi:10.1007/s12035-016-0072-3.

[12] Guzowski JF, McGaugh JL. Interaction of neuromodulatory systems regulating memory storage. In: Decker M, Brioni JD, editors. Alzheimer's disease: molecular aspects and pharmacological treatments. Hoboken: Wiley-Liss; 1997. p. 37–61.

[13] Miyashita T, Kubik S, Lewandowski G, Guzowski JF. Networks of neurons, networks of genes: an integrated view of memory consolidation. Neurobiol Learn Mem 2008;89:269–84. doi:10.1016/j.nlm.2007.08.012.

[14] An L, Zhang T. Vitamins C and E reverse melamine-induced deficits in spatial cognition and hippocampal synaptic plasticity in rats. Neurotoxicology 2014;44:132–9. doi:10.1016/j.neuro.2014.06.009.

[15] Wu A, Ying Z, Gomez-Pinilla F. Vitamin E protects against oxidative damage and learning disability after mild traumatic brain injury in rats. Neurorehabil Neural Repair 2010;24:290–8. doi:10.1177/1545968309348318.

[16] Lee B, Shim I, Lee H, Hahm DH. Effects of epigallocatechin gallate on behavioral and cognitive impairments, hypothalamic-pituitary-adrenal axis dysfunction, and alternations in hippocampal BDNF expression under single prolonged stress. J Med Food 2018;21:979–89. doi:10.1089/jmf.2017.4161.

[17] Zhang ZS, Qiu ZK, He JL, Liu X, Chen JS, Wang YL. Resveratrol ameliorated the behavioral deficits in a mouse model of post-traumatic stress disorder. Pharmacol Biochem Behav 2017;161:68–76. doi:10.1016/j.pbb.2017.09.004.

[18] Takeda M, Nagano K, Kuroda H, Hirai H, Maekita H, Harada K, et al. Absorption analysis of amorphous cucumin to develop functional foods with high quality. In: Congress proceeding of the 137th of the Annual Meeting of the Pharmaceutical Society of Japan. 26 PB pm107S; 2017. p. 218. March 24th-27th, 2017.

[19] Monsey MS, Gerhard DM, Boyle LM, Briones MA, Seligsohn M, Schafe GE. A diet enriched with curcumin impairs newly acquired and reactivated fear memories. Neuropsychopharmacology 2015;40:1278–88. doi:10.1038/npp.2014.315.

[20] Milad MR, Igoe SA, Lebron-Milad K, Novales JE. Estrous cycle phase and gonadal hormones influence conditioned fear extinction. Neuroscience 2009;164:887–95. doi:10.1016/j.neuroscience.2009.09.011.
[21] Pawluski JL, Brummelte S, Barha CK, Crozier TM, Galea LA. Effects of steroid hormones on neurogenesis in the hippocampus of the adult female rodent during the estrous cycle, pregnancy, lactation and aging. Front Neuroendocrinol 2009;30:343–57. doi:10.1016/j.yfrne.2009.03.007.
[22] von Bohlen Und Halbach O. Immunohistological markers for staging neurogenesis in adult hippocampus. Cell Tissue Res 2007;329:409–20. doi:10.1007/s00441-007-0432-4.
[23] Iosif RE, Ekdahl CT, Ahlenius H, Pronk CJ, Bonde S, Kokaia Z, et al. Tumor necrosis factor receptor 1 is a negative regulator of progenitor proliferation in adult hippocampal neurogenesis. J Neurosci 2006;26:9703–12. doi:10.1523/JNEUROSCI.2723-06.2006.
[24] Brami-Cherrier K, Roze E, Girault JA, Betuing S, Caboche J. Role of the ERK/MSK1 signalling pathway in chromatin remodelling and brain responses to drugs of abuse. J Neurochem 2009;108:1323–35. doi:10.1111/j.1471-4159.2009.05879.x.
[25] Tzingounis AV, Nicoll RA. Arc/Arg3.1: linking gene expression to synaptic plasticity and memory. Neuron 2006;52:403–7. doi:10.1016/j.neuron.2006.10.016.
[26] Paxinos G, Watson C. The rat brain in stereotaxic coordinates. 7th ed. London, Waltham, San Diego: Academic Press; 2014.
[27] Kovács KJ. Measurement of immediate-early gene activation- c-fos and beyond. J Neuroendocrinol 2008;20:665–72. doi:10.1111/j.1365-2826.2008.01734.x.
[28] Okada R, Masubuchi Y, Tanaka T, Nakajima K, Masuda S, Nakamura K, et al. Continuous exposure to α-glycosyl isoquercitrin from developmental stage facilitates fear extinction learning in rats. J Funct Foods 2019;55:312–24. doi:10.1016/j.jff.2019.02.024.
[29] Livak KJ, Schmittgen TD. Analysis of relative gene expression data using real-time quantitative PCR and the $2^{-\Delta\Delta C}{}_T$ method. Methods 2001;25:402–8. doi:10.1006/meth.2001.1262.
[30] Sterlemann V, Ganea K, Liebl C, Harbich D, Alam S, Holsboer F, et al. Long-term behavioral and neuroendocrine alterations following chronic social stress in mice: implications for stress-related disorders. Horm Behav 2008;53:386–94. doi:10.1016/j.yhbeh.2007.11.001.
[31] Stone SS, Teixeira CM, Zaslavsky K, Wheeler AL, Martinez-Canabal A, Wang AH, et al. Functional convergence of developmentally and adult-generated granule cells in dentate gyrus circuits supporting hippocampus-dependent memory. Hippocampus 2011;21:1348–62. doi:10.1002/hipo.20845.
[32] Yochiy A, Britto LR, Hunziker MH. Novelty, but not operant aversive learning, enhances Fos and Egr-1 expression in the medial prefrontal cortex and hippocampal areas of rats. Behav Neurosci 2012;126:826–34. doi:10.1037/a0030721.
[33] Fleischmann A, Hvalby O, Jensen V, Strekalova T, Zacher C, Layer LE, et al. Impaired long-term memory and NR2A-type NMDA receptor-dependent synaptic plasticity in mice lacking c-Fos in the CNS. J Neurosci 2003;23:9116–22. doi:10.1523/JNEUROSCI.23-27-09116.2003.
[34] Vidal-Gonzalez I, Vidal-Gonzalez B, Rauch SL, Quirk GJ. Microstimulation reveals opposing influences of prelimbic and infralimbic cortex on the expression of conditioned fear. Learn Mem 2006;13:728–33. doi:10.1101/lm.306106.
[35] Harney SC, Jane DE, Anwyl R. Extrasynaptic NR2D-containing NMDARs are recruited to the synapse during LTP of NMDAR-EPSCs. J Neurosci 2008;28:11685–94. doi:10.1523/JNEUROSCI.3035-08.2008.
[36] Pape HC, Pare D. Plastic synaptic networks of the amygdala for the acquisition, expression, and extinction of conditioned fear. Physiol Rev 2010;90:419–63. doi:10.1152/physrev.00037.2009.
[37] Eadie BD, Cushman J, Kannangara TS, Fanselow MS, Christie BR. NMDA receptor hypofunction in the dentate gyrus and impaired context discrimination in adult Fmr1 knockout mice. Hippocampus 2012;22:241–54. doi:10.1002/hipo.20890.
[38] Schurmans S, Schiffmann SN, Gurden H, Lemaire M, Lipp HP, Schwam V, et al. Impaired long-term potentiation induction in dentate gyrus of calretinin-deficient mice. Proc Natl Acad Sci U S A 1997;94:10415–20. doi:10.1073/pnas.94.19.10415.
[39] Lin X, Bai D, Wei Z, Zhang Y, Huang Y, Deng H, et al. Curcumin attenuates oxidative stress in RAW264.7 cells by increasing the activity of antioxidant enzymes and activating the Nrf2-Keap1 pathway. PLoS One 2019;14:e0216711. doi:10.1371/journal.pone.0216711.
[40] Love S. Oxidative stress in brain ischemia. Brain Pathol 1999;9:119–31. doi:10.1111/j.1750-3639.1999.tb00214.x.
[41] Jing W, Chunhua M, Shumin W. Effects of acteoside on lipopolysaccharide-induced inflammation in acute lung injury via regulation of NF-κB pathway in vivo and in vitro. Toxicol Appl Pharmacol 2015;285:128–35. doi:10.1016/j.taap.2015.04.004.
[42] Babri S, Doosti MH, Salari AA. Tumor necrosis factor-alpha during neonatal brain development affects anxiety- and depression-related behaviors in adult male and female mice. Behav Brain Res 2014;261:305–14. doi:10.1016/j.bbr.2013.12.037.
[43] Kim SJ, Son TG, Park HR, Park M, Kim MS, Kim HS, et al. Curcumin stimulates proliferation of embryonic neural progenitor cells and neurogenesis in the adult hippocampus. J Biol Chem 2008;283:14497–505. doi:10.1074/jbc.M708373200.
[44] Ekdahl CT, Kokaia Z, Lindvall O. Brain inflammation and adult neurogenesis: the dual role of microglia. Neuroscience 2009;158:1021–9. doi:10.1016/j.neuroscience.2008.06.052.
[45] Robinson BV, Sullivan FM, Borzelleca JF, Schwartz SL. Toxicological studies on PVP. In: PVP: a critical review of the kinetics and toxicology of polyvinylpyrrolidone (Povidone). Boca Raton, London, New York: CRC Press; 1990. p. 121–45.